Master's thesis

NTNU
Norwegian University of Science and Technology
Faculty of Engineering
Department of Marine Technology

Martin Mongstad Hope

Offshore Towing of Floating Wind Turbines design aspects with focus on numerical modelling

Master's thesis in Marine Technology
Supervisor: Kjell Larsen
June 2021

NTNU
Norwegian University of Science and Technology

Martin Mongstad Hope

Offshore Towing of Floating Wind Turbines design aspects with focus on numerical modelling

Design av offshore taueoperasjoner av flytende vindturbiner – numeriske simuleringer

Master's thesis in Marine Technology
Supervisor: Kjell Larsen
June 2021

Norwegian University of Science and Technology
Faculty of Engineering
Department of Marine Technology

NTNU
Norwegian University of
Science and Technology

NTNU Trondheim
Norges teknisk-naturvitenskapelige universitet
Institutt for marin teknikk

MASTER THESIS SPRING 2021
for

Stud. tech. Martin Mongstad Hope

Offshore Towing of Floating Wind Turbines – design aspects with focus on numerical modelling

Design av offshore taueoperasjoner av flytende vindturbiner – numeriske simuleringer

Background

Towing operations are the most common marine operation. It is defined as a transport of a self-floating object by one or several towing tugs. It includes towing of self-floating objects and large structures, objects on transportation barges, emergency towing (e.g. icebergs) and towing of long, slender objects (pipes and bundles). These operations are associated with considerable risk; lack of planning and risk understanding have resulted in several losses of towed objects, many due to towline failures.

The offshore wind industry is moving into deeper water and farther from land where floating wind turbines (FWTs) become more economical than bottom-fixed units. The cost of marine operations for single units and future wind farms will become a large part of the total cost for such developments. Safe and smart execution of all types of marine operations is therefore a key enabler for FWTs. In this project, the offshore towing operations for a single FWT shall be studied. The Hywind Tampen project is selected as the main case.

Some important challenges for typical towing operations comprise
- Tow global behavior (motions) and load effects in towing lines due to environmental loads from wind, waves and ocean current.
- Requirements to tugboats and towing equipment.
- Planning of operation in terms of limiting weather conditions and weather routing and safe havens.
- Understanding and managing the risks – severe accidents and loss of towed objects are too often experienced.

Scope of Work

1) Review relevant literature and
- describe state-of-art concepts for offshore towing.
- describe selected towing accidents using information in public domain and pinpoint direct causes and consequences.

2) Describe the steps in the planning process of a towing operation. Explain the differences in "weather restricted" and "weather unrestricted" towing and how weather windows and operability can be estimated. Give a brief overview of the Hywind Tampen project. Include the different fabrication steps and the marine operations related to the different steps. Consider the towing operations to be performed and give rough estimates of planned operation times.

3) Give an overview of the design methodology and the split between static and dynamic load effects in a typical towing operation involving one ship-shaped tugboat and the Hywind Tampen FWT. Environmental models of load effects from wind, current and waves relevant for tow motion behavior and towline tension shall be described. Describe the models for the tugboat and the Hywind Tampen FGWT and complete the input data for a numerical simulation model to be used in SIMO and RIFLEX.

4) Establish and compare several numerical simulation models of a tugboat towing an assembled FWT for the Hywind Tampen project. Start with a simple quasi-static model of the tugboat and towing line and extend the model stepwise in SIMO by making models for towing line and Hywind Tampen. Improve the model by establishing a coupled SIMO/RIFLEX model where a dynamic model of the towing line is included in RIFLEX. Models and cases to be discussed and agreed with supervisor.

5) Perform numerical simulations using the different models established in 4). Discuss and compare the performance focusing on vessel motions and towing line tensions. Propose a model to be used in future assessment of such operations.

6) Conclusions and recommendations for further work.

General information

All necessary input data for the simulation case is assumed to be provided by NTNU/Equinor. The work scope may prove to be larger than initially anticipated. Subject to approval from the supervisor, topics may be reduced in extent.
In the thesis report, the candidate shall present his personal contribution to the resolution of problems within the scope of work.
Theories and conclusions should be based on mathematical derivations and/or logic reasoning identifying the various steps in the deduction.
The candidate should utilise the existing possibilities for obtaining relevant literature.

Report/Delivery
The thesis report should be organised in a rational manner to give a clear exposition of results, assessments, and conclusions. The text should be brief and to the point, with a clear language. Telegraphic language should be avoided.

The report shall be written in English and edited as a research report including literature survey, description of relevant mathematical models together with numerical simulation results, discussion, conclusions and proposal for further work. List of symbols and acronyms, references and (optional) appendices shall also be included. All figures, tables and equations shall be numerated.

The original contribution of the candidate and material taken from other sources shall be clearly defined. Work from other sources shall be properly referenced using an acknowledged referencing system.

The report shall be submitted in Inspera, as specified by the department of Marine Technology. In addition, an electronic copy (pdf) to be sent to the supervisor.

Ownership
NTNU has according to the present rules the ownership of the project results. Any use of the project results has to be approved by NTNU (or external partner when this applies). The department has the right to use the results as if the work was carried out by a NTNU employee, if nothing else has been agreed in advance.

Thesis supervisor**:**
Prof. II Kjell Larsen, NTNU/Equinor

Deadline: June 10th , 2021

Trondheim, January 26th, 2021

Kjell Larsen (sign)

Martin Mongstad Hope (sign)

Preface

This master thesis has been written by the author during the spring semester of 2021 during the 5th and final year of a 5 year integrated Master's Degree in Marine Technology at the Department of Marin Technology, Norwegian University of Science and Technology (NTNU). The thesis about marine towing operation has been carried out at NTNU with a workload corresponding to 30 ECTS. This thesis continues the work from my project thesis written the autumn semester of 2020 with a workload corresponding to 7.5 ECTS

Acknowledgement

I would like to express my sincere gratitude to my supervisor for this thesis Professor II Kjell Larsen. Frequent meetings have been of great help in understanding the project, and his knowledge regarding marine operations has been of a great help in understanding the surrounding theory. I would also like to thank Erling Neerland Lone and Gro Sagli Baarholm for their help and guidance with regards to SIMA.

Trondheim, 2021-06-10

Martin Mongstad Hope

Abstract

This master thesis on dynamic analysis of marine towing operations, seeks to propose a model to be used for assessing the dynamic tension in a towing line. Four different models has been evaluated, one uses a quasistatic frequency response analysis. While the other three uses time domain analysis. Two of the time domain models uses separation of motions while the third use total motion in order to determine the motions of the towing vessel. One of the separation of motion models uses quasistatic analysis and the second, uses a simplified dynamic analysis accounting for the effect of drag loading on the line. In order to model the towline. The total motion model uses a coupled FEA model to model the towing line. In order to carry out the frequency model analysis Matlab is used, while the time domain analysis uses SIMA. The separation of motion models uses SIMO while the total motion analysis uses a couple SIMO/RIFLEX model. As a part of this a literature review on the state-of-art concepts for offshore towing and selected towing accidents.

Sammendrag

Denne master oppgaven på dynamisk analyse av marine taue operasjoner, søker å foreslå en modell for vurdering av det dynamisk streke i ei taueline. Fire ulike modeller har blitt evaluert, en av modellen bruker en kvasistatisk frekvens respons analyse. Mens de resterende tre modellene bruker tids domene analyse. To av tids domen modellene bruker seperasjon av bevegelse får å fastslå bevegelsen til taubåten, mens den tredje bruker total bevegelse. For modellen som bruker seperasjon av bevegelse En av modellen som bruker seperasjon av bevegelse modellerer taulina ved bruk av kvasistatisk analyse, mens den andre bruker en simplifisert dynamisk analyse. Den simplifiserte dynamisk analysen regner med motstands kraften på lina. For å modeller taulina total motion modellen bruker en kobla FEA model. Frekvens domene analysen blei utfør i Matlab, mens tids domene analysen blei utført i SIMA. For separasjon av bevegelse analyse blir en rein SIMO model brukt, mens for total bevegelse analysen brukes en kobla SIMO/RIFLEX modell. Som en del av dette et litteratursøk på moderne konsepter for offshore tauing og utvalgte taue ulykker.

Contents

Figures

Tables

Nomenclature

$\boldsymbol{A}(\omega)$	Frequency-dependent added mass matrix
$\boldsymbol{C}(\omega)$	Frequency-dependent potential damping matrix
$\boldsymbol{D}_{\mathrm{l}}$	Linear damping matrix
$\boldsymbol{D}_{\mathrm{q}}$	Quadratic damping matrix
$\boldsymbol{K}(\eta)$	Hydrostatic and towline stiffness matrix
$\boldsymbol{m}$	Body mass matrix
$\boldsymbol{X}_{hf}$	First order transfer function between motion and wave elevation
Δ	Mass displacement of the tug
η	shape factor
η_{ϕ}	Motion along towline
$\eta_{1_{AP}}$	Surge motion at attachment point
$\eta_{1_{COG}}$	Surge motion at centre of gravity
$\eta_{2_{AP}}$	Sway motion at attachment point
$\eta_{2_{COG}}$	Sway motion at centre of gravity
$\eta_{3_{AP}}$	Heave motion at attachment point
$\eta_{3_{COG}}$	Heave motion at centre of gravity
$\eta_{4_{COG}}$	Roll motion at centre of gravity
$\eta_{5_{COG}}$	Pitch motion at centre of gravity
$\eta_{6_{COG}}$	Yaw motion at centre of gravity
$\overline{T}$	Mean tension in towing line
$\overline{U}$	Mean wind velocity

ρ_a	Density of air
ρ_w	Density of water
τ_c	Duration of calm
$\theta_{1_{COG}}$	Phase of the surge motion at centre of gravity
$\theta_{2_{COG}}$	Phase of the sway motion at centre of gravity
$\theta_{3_{COG}}$	Phase of the heave motion at centre of gravity
$\theta_{4_{COG}}$	Phase of the roll motion at centre of gravity
$\theta_{5_{COG}}$	Phase of the pitch motion at centre of gravity
$\theta_{6_{COG}}$	Phase of the yaw motion at centre of gravity
$\vec{\ddot{\eta}}$	Acceleration vector
$\vec{\ddot{\eta}}_{hf}$	High frequency acceleration vector
$\vec{\ddot{\eta}}_{lf}$	Low frequency acceleration vector
$\vec{\dot{\eta}}$	Velocity vector
$\vec{\dot{\eta}}_{hf}$	High frequency velocity vector
$\vec{\dot{\eta}}_{lf}$	Low frequency velocity vector
$\vec{\eta}$	Position vector
$\vec{\eta}_{hf}$	High frequency position vector
$\vec{\eta}_{lf}$	Low frequency position vector
$\vec{q}_{cu}$	current drag force vector
$\vec{q}_{ext}$	Any other forces vector
$\vec{q}^1_{wa}(t)$	first order wave excitation force vector
$\vec{q}^2_{wa}(t)$	second order wave excitation force vector
$\vec{q}_{wi}(t)$	wind drag force vector
$\vec{V}_r$	Relative velocity vector
ζ_a	Wave amplitude
$\overline{V}$	Mean current velocity
$A_{exp_{tow}}$	projected cross-sectional area of towed object

BP	Continuous static bollard pull of the vessel in tonnes
$c(\omega)$	mean wave drift force coefficient
c_{cu}	Drag coefficient current
C_{drag}	Linearized damping coefficient due to drag on towline
C_D	Drag coefficient
$c_{wi_{tower}}$	Drag coefficient wind for tower
c_{wi}	Drag coefficient wind
D_{dry}	Dry diameter of the turbine
D_{line}	Diameter of the towing line
D_{wet}	Wet diameter of the turbine
E	Modulus of elasticity
f	Amplification facto
F_{cu}	Current force
F_p	Propeller thrust
F_{r0}	Resistance towed object
F_{rt}	Resistance tug
F_r	Total Resistance
F_{TD}	Towline design load in tonnes
F_{wd}	Wave drift force
F_{wi}	Wind force
H_s	Significant wave height
$L_{towline}$	Length of towline
OP_{WF}	Operational Criterion
$S(\omega)$	JONSWAP spectrum
T_{η_3}	Eigen period in heave for the tug
T_{η_4}	Eigen period in Roll for the tug
T_{η_5}	Eigen period in Pitch for the tug

T_0	Tension in towing line
T_1	Mean wave period
T_a	Amplitude of dynamic tension in towline
T_{b0}	Towing force
T_{b1}	Force in port bridle
T_{b2}	Force in starboard bridle
T_D	Tension in the towing line due to drag
T_d	Return Period
T_{op}	Total Operational Time
T_p	Mean wave period
T_R	Operation Reference Period
$T_{tot_{MPM}}$	Most probable maximum tension in towing
T_{tot}	Total Available Time
u(t)	dynamic wind gust velocity
U_{10}	Mean wind speed at 10 m above sea level
u_a	Amplitude of towing line motion causing geometric change and drag
V_{rc}	Relative velocity wind
V_{rwi}	Relative velocity current
w	submerged weight per unit length
w_0	weight per unit length of the towline in unstretched condition
x_a	Amplitude of vessel motion

Chapter 1

Introduction

1.1 Background

Towing operations are the most common marine operation. And is associated with many incidents,partly due to towline failure caused by lack of planning and risk understanding. As the offshore industry, moves into deeper water and farther from land the operational time increases. Due to this the cost also increases. For some industries such as offshore wind the the cost of marine operations becomes a large part of the total cost of development. In this thesis offshore towing of an assembled floating wind turbine (FWT) shall be studied further.

1.2 Objectives

The overall goal of this thesis is to establish and compare several numerical simulation models of a tugboat towing an assembled FWT for the Hywind Tampen project. The objectives of this thesis are:

1. Describe state-of-art concepts for offshore towing.
2. Give an overview of some relevant towing accidents and pinpoint direct causes and consequences.
3. Describe the steps in the planning process of a towing operation. Explain the differences in “weather restricted” and “weather unrestricted” towing and how weather windows and operability can be estimated.
4. Give a brief overview of the Hywind Tampen project
5. Give an overview of the design methodology for a typical towing operation involving one ship-shaped tugboat and the Hywind Tampen FWT.
6. Perform calculations of static forces on the involved vessels and indicate the need for tugboat capacity and towline dimensions. Using relevant weather data for the Tampen area.
7. Establish and compare several numerical simulation models of a tugboat towing an assembled FWT for the Hywind Tampen project.
8. Perform numerical simulations using the different models established

9. Discuss and compare the performance focusing on vessel motions and towing line tensions.
10. Propose a model to be used in future assessment of such operations.
11. Conclusions and recommendation for further work

1.3 Structure of the Report

The rest of the thesis is organised as follows.

Chapter 2 gives an introduction to state of the art concepts in offshore towing. Following that is gives an overview of some towing accidents, and some typical failure modes in towing lines. It also describes the steps in the planing process of a towing operation. Finally it gives an overview of weather restricted and unrestricted operation and weather windows and operability.

Chapter 3 Gives an overview of the design methodology and the split between static and dynamic load effects.

Chapter 4 Gives a brief description of the Hywind Tampen project. Then it descries the models for the tugboat and FWT. Finally it describes the weather conditions used in the analysis of the dynamic tension.

Chapter 5 Describes the models used to in the analysis and presents and discuses their results.

In Chapter 6 summary and conclusions are given along with recommendations for further work.

Chapter 2

Marine Towing

Towing is the most common marine operation and is a part of most offshore development projects. It is a non-routine operation of a limited duration related to handling of object(s) and/or vessel(s) in the marine environment during temporary phases. Towing operations shall be planned according to safe and sound practice, and according to defined codes and standards. They shall also be designed to bring the object from one defined safe condition to another safe condition. "Safe Condition" is defined as a condition where the object is considered exposed to normal risk (i.e. similar risk as expected during in-place condition) for damage or loss. [1]. To achieve this requires careful planing. The planing is complicated by the fact that no towing operation is exactly the same. Some examples of tow operations are listed below:

- Rig move
- Transport to or between sites of large floating structure
- Transport of object on separate barge
- Wet tow of long slender structures
- Wet tow of subsea modules

2.1 Towing configurations

Table 2.1 shows different towing configurations as given in DNV-OS-H202. Other towing configurations than normal and parallel may only be used after a risk assessment of each case considering the actual tow arrangement, towed objects, route and season. Required bollard pull and manoeuvrability are two of the factors effecting the choice of towing configuration, along with the shape and type of object being towed. The goal is to ensure proper control over the towed object.

- Normal tow: One tug towing one object.
- Parallel tow: Two or more tugs in parallel. Each tug is connected by its own towline to the same towed object.
- Double tow: Two towed objects each connected to the same tug with separate towlines. One of the towlines is of sufficient length to pass well below

Table 2.1: Towing configurations [2]

Tugs		Objects		Tow called (see notes)
No.	Position	No.	Position	
1	NA	1	NA	Normal
2 or more	Parallel	1	NA	Parallel
2	Series	1	NA	Serial
3 or more	Series	1	NA	
1	NA	2	Parallel	Double
1	NA	3 or more	Parallel	
1	NA	2 or more	Series	Tandem

the first towed object.

- Tandem tow: Two towed objects in series behind one tug, i.e. the second object is connected to the stern of the first object.
- Serial tow: Two tugs in series. The towed object is connected to the second tug and this tug is connected to the leading tug

2.1.1 Surface Tow of Large Structures

The wind turbines for Hywind Tampen is an example of surface tows of large volume objects. Figure 2.1 shows classical towing configurations. he top and bottom configurations are of particular interest for offshore operations. For towing barges and wind mils the top configuration is used, and for large platforms the bottom configuration is used. The middle configuration is applicable for towing in restricted waters such as narrow water ways and not for open ocean towing.

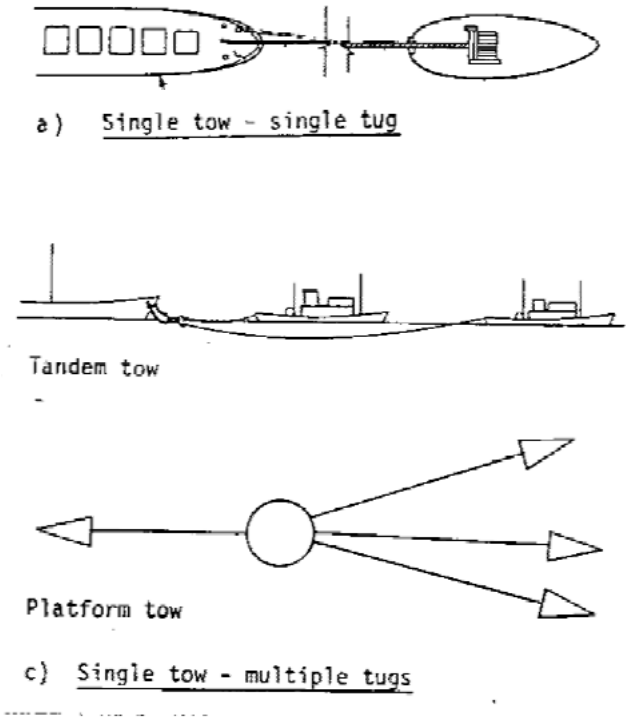

Figure 2.1: Classical towing configurations,[3]

Inshore/Restricted Tow

During inshore/restricted towing manoeuvrability is the most important consideration. In order to account for this the towing lines are short and the tugs are located to easily apply forces in any direction. Figure 2.2 shows an example of a towing configuration for a restricted tow.

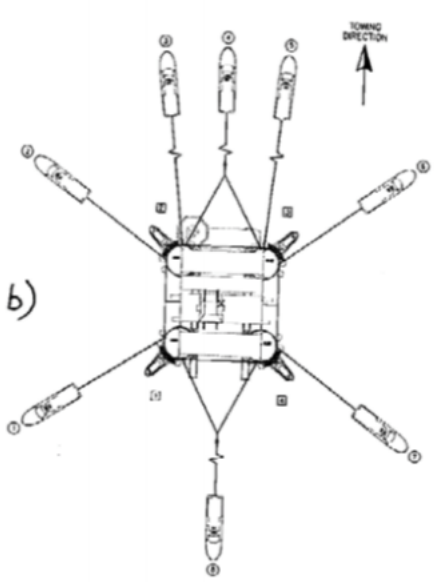

Figure 2.2: Inshore towing configuration for the Heidrun platform,[4]

Offshore Tow

For offshore tows towing speed and loads in the towing lines are important considerations. The towing speed is important in order to minimise the towing duration in order to save costs and increased operability for weather restricted operations due to a smaller required weather window. The tugs are arranged to allow the most thrust in the same direction. Figure 2.3 shows an example of a towing configuration for a offshore tow.

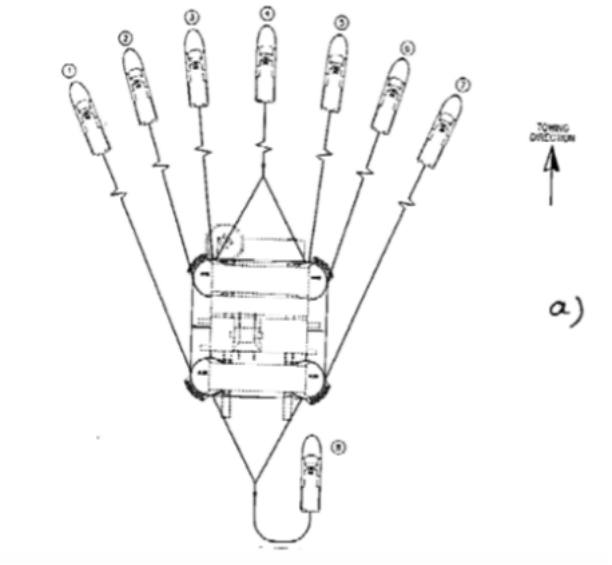

Figure 2.3: Offshore towing configuration for the Heidrun platform,[4]

2.1.2 Submerged Tow

Modern subsea equipment will often require large deck space and crane capacity in order to improve fleet utilisation submerged towing may be used. Submerged towing may also increase operability by avoiding offshore operations with low limiting criteria such as lifting off barges and/or lowering through the splash zone. DNV-RP-H103 [5] gives the following examples of critical parameters to be considered in modelling and analysis of a submerged tow

- vessel motion characteristics
- wire properties
- towing speed
- routing of tow operation (limited space for manoeuvring, varying current condition)
- directional stability of towed object as function of heading
- forces in hang-off wire, slings and towing bridle
- clearance between object and tow vessel
- clearance between rigging and vessel
- VIV of pipe bundles and slender structures (e.g. spools, structure/piping)
- lift effects on sub-surface towed structures
- wave loads on surface towed bundles (extreme and fatigue loading).

The Pencil Buoy Method The Pencil Buoy Method (PBM) is designed for transportation and installation of subsea structures. The structure is transported to a inshore transfer location nearby the installation cite by a crane barge. It is then lifted true the splash zone, before the structure weight it transferred from the crane barge to an Installation Vessel (IV). The structure rigging will be con-

nected to IV's winch wire and a tubular buoyancy tank (pencil buoy). The pencil buoy is then launched from IV deck by paying out of the towing winch while IV moves slowly forward. The structure and the rigging weight are carried by the Pencil Buoy during tow. Figure 2.4 shows an example of the pencil buoy set-up during tow. Normally a tow speed of 3 - 3.5 knots is used and has weight capacity of 350 tonnes [6].

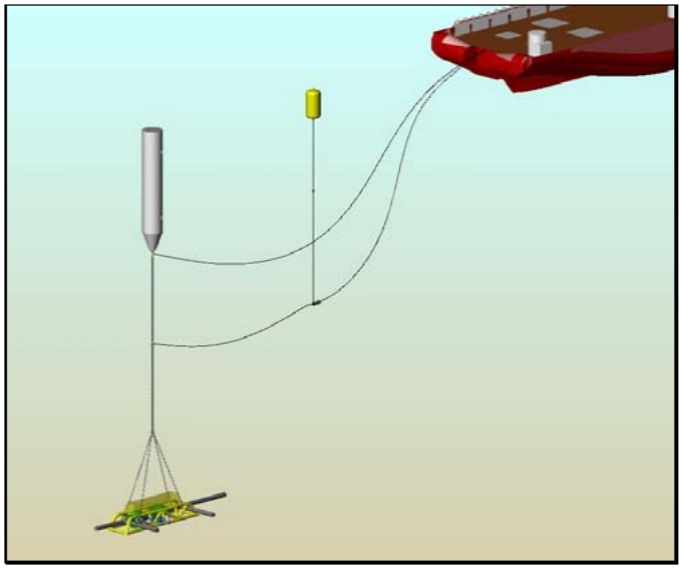

Figure 2.4: Pencil Buoy Method Set-Up,[6]

Objects Attached to Vessel

The object is picked up from wet-store using a winch system, and connected to the towing vessel. Figure 2.5 shows an example of the attachment configuration. The object can hang in a rigging arrangement through the moon pool of the vessel, but it requires that particular attention is given to check clearance between rigging and moon pool edges.

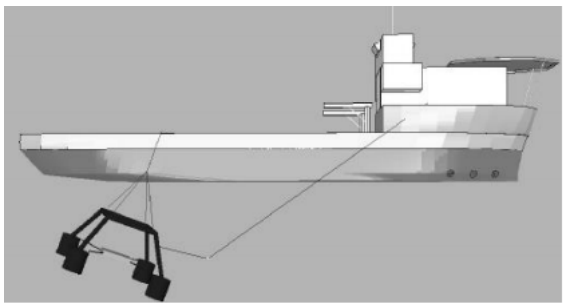

Figure 2.5: Submerged object attached to vessel,[5]

2.1.3 Towing of slender structures

Towing of long slender objects are normally done by one of the following methods:

1. Surface Tow
2. Near surface Tow
3. Bottom Tow
4. Off-bottom Tow
5. Controlled Depth Tow (CDT)

Regardless of which of the method is used the main feature of restriction is the limited length of pipe that can be towed. When towing slender objects several may be towed together as a bundle (strapped together or within a protective casing).

Surface and near surface tows is used for both short and long distance tows. This method allows for the pipe to be fabricated on land, launched and towed to location in a single length. It is more weather dependent due to the towed object being influenced by waves.

Bottom tow has been extensively employed on marine pipeline projects, and has established an excellent reliability record. This method typicality employs winches at fixed locations such as onshore, on anchored barges, and on platforms where it has been used to perform tie-ins [7].

Off-bottom tow may be considered as a variation of the bottom tow method. Where the pipeline is floating at a uniform height off the seabed. Off-bottom tow uses a combination of buoyancy and ballast chains so that the towed object is elevated above the seabed. The ballast chains are used to ensure sufficient submerged weight and stability. The bouancy may be provided by the buoyancy of the pipeline itself, or by pontoons or floats attached to the line.

CDT is a further development of the off-bottom tow method By careful design of towline length, holdback tension, buoyancy, ballast and drag chains, the towed object will be lifted off the seabed at a critical tow speed to be towed at a 'controlled depth' above obstructions on the sea bed, but below the area with strong wave influence. Both the tow vessel at the front and the holdback vessel at the rear continuously apply tension to the pipe throughout tow-out. Figure 2.6 and 2.7 shows illustrations of the different methods for towing slender elements.

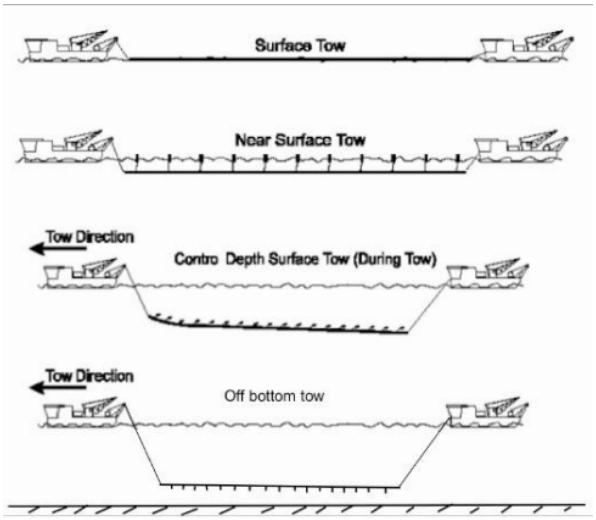

Figure 2.6: Different methods for tow of long slender objects, [8]

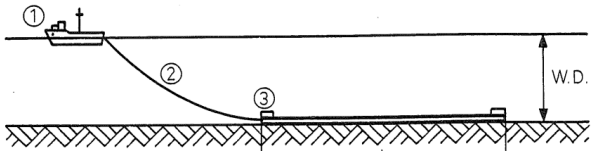

Figure 2.7: Bottom tow, [7]

2.2 Accidents

Figure 2.8 shows the statistics of 89 towline breakages, the data is old but valid, [8]. The figure shows that most failures are in the synthetic fibre and at the stern of the tug, and that the main reasons for these towline failure are overload, wear fatigue and propeller cutting [8].

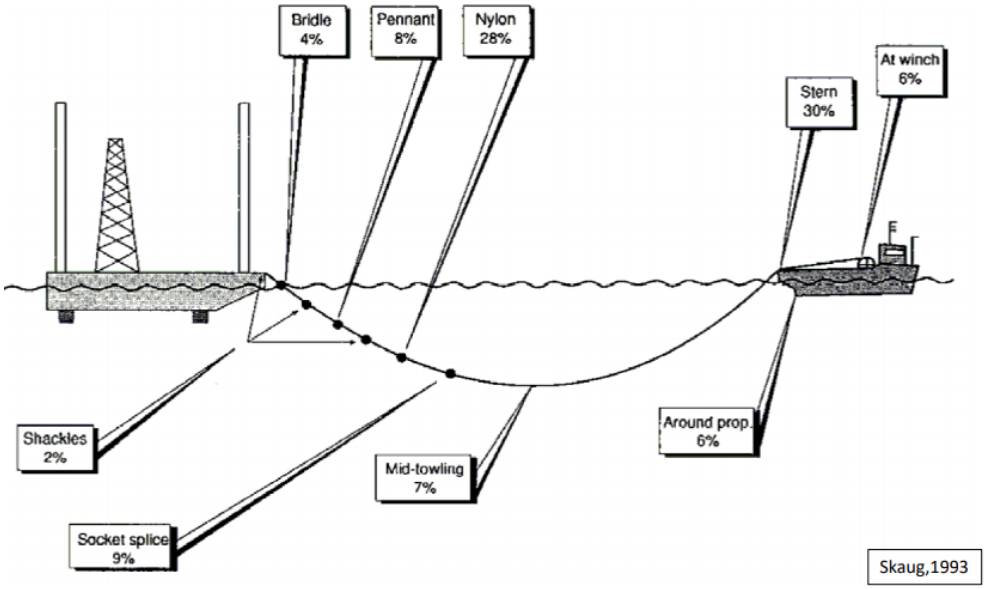

Figure 2.8: Statistics of line breakage. Based on 89 towline breakages,[9]

Table 2.2 gives some examples of accidents focusing on causes and consequences. In the following a more detailed overview of an accidents will be given.

Table 2.2: Examples of some towing accidents, [10] [11]

Vessel	Year	Location	Description	Consequences
Retainer	2007	England	The most likely cause of the accident was due to one of the tow ropes becoming snagged on the forward section of the barge. When the snag cleared,it transmitted a wave along the tow rope which caught a crewmember in the chest with significant force	1 Fatality.
Englishman	2008	England	A tow wire protector used to prevent wire chafing on the bulwark rail slipped outboard of the bulwark rail. While trying to reposition, the wire jumped, hitting a crewman in the head.	1 Fatality.
Magadan and Neftegaz-55	2011	Russia	During the tow of the jack-up rig Kolskaya the weather changed to gale force winds and 5-6 m high waves. Due to failure of tank air inlets resulted in seawater filing the tanks. At the same time the tow-line from the Magadan was damaged due to heavy loads. After som time the rig capsized.	53 Fatalities and the Jack up rig Kolskaya capsized.
ALP Forward	2016	Scotland	The tug and tow was on passage from Stavanger, Norway to Valletta, Malta when it encountered severe weather west of the Hebrides. The effect of the wind and waves on Transocean Winner led to the loss of ALP Forward's ability to control the direction and speed of the tug and tow. After being dragged backwards by the tow for over 24 hours, the tow line, weakened by the repeated sudden loadings, parted and the tug was unable to pick up the emergency towline.	A The semi-submersible rig Transocean Winner grounded on the Isle of Lewis

2.2.1 Kulluk accident

The following is based on information from [11]. The drilling rig Kulluk was towed from Dutch Harbor to Seattle for winter maintenance during December 2012. The 1700 nm tow was started despite a metocean forecast of harsh weather. None of the deck officers on the towing vessel Aiviq had experience towing in Alaskan waters. In the hours before the accident an alarm set for activation at 50% of the strength limit of the tow equipment went of 38 times. During this time the towing line length was increased multiple times in order to try to lower the tension.

Figure 2.9 shows a time line linking the overload alarms with operation of the wire made by the United States Coast Guard. A shackle eventually failed and the towline was lost. The weather did not allow for resetting the towing gear with cranes. A emergency towing wire was established, but failed fairly soon. A few hours later the towing vessel lost all of its four main engines. The rig then drifted out of control until it grounded near Kodiak.

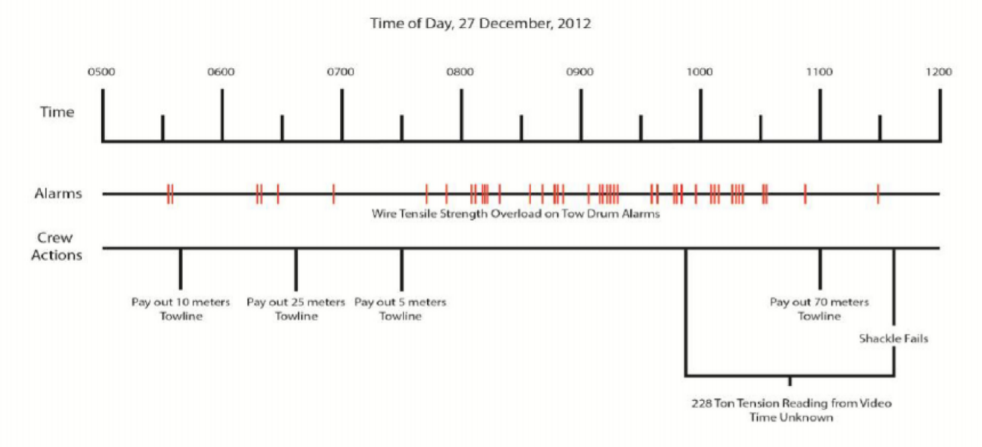

Figure 2.9: Analysis of "Wire Tensile Strength Overload on Tow Drum Alarms" and crew actions with respect to towline operation, [12]

The direct cause of this accident was shackle failure due to heavy loads resulting in the consequences of engine failure in the tug and grounding of the drilling rig. But the risk management practices of the companies involved were highlighted as one of the principal causes of the accident, in an accident report by the United States Coast Guard. The lack of Arctic operational experience of the officers on the towing vessel was also highlighted as an important factor.

2.3 Planning process

Marine operations shall be planned according to fail safe principles [4]. They shall be designed to bring an object from one defined safe condition to another. While planning d according to safe and sound practice, and according to defined codes and standards. In DNV-OS-H101 [1] DNV recommends the following planing process, while considering planing and design as an iterative process:

1. Identify relevant and applicable regulations, rules, company specifications, codes and standers, both statutory and self-elected
2. Identify physical limitations
3. Overall planning of operation i.e. evaluate operational concepts, and physical limitations applicable for the operation
4. Develop design basis describing environmental conditions and physical limitations applicable for the operation

5. Develop briefs describing activities planned in order to verify the operation, i.e. available tools planned analysis including method and particulars, applicable codes, acceptance criteria, etc.
6. Carry out engineering and design analyses
7. Develop operation procedures

The marine operations should be planed with a probability for structural failure less than 1/10000 per operation ($10^{-}4$-probability). Note that above stated probability level defines a structural capacity reference. When also considering the probability of operational errors, the total probability of failure may increase [1].

Marine operations are generally separated into two categories weather restricted and weather unrestricted. Weather restricted operations shall be of a limited duration normally less than 72 hours. This allows operations to be designed and planned for a considerably lower environmental condition than the seasonal, statistical extremes used for an unrestricted operation. Due to this the restricted operation needs to take place within the limits of a favourable weather forecast related to the selected design environmental condition for the operation. Weather unrestricted operations on the other hand is design base on statistical extremes for the area and season. They should be able to take place safely in any weather condition that can be encountered during the season. Table 2.3 shows the required return periods of waves for different operation lengths. Weather restricted operation normally have a planned operation time longer than 72 hours but can be shorter.

Table 2.3: Acceptable return periods for H_s, [1]

Reference Period, T_R	Return Period, T_d
$T_R \leq 3$ days	$T_d \geq 1$ month
3 days $< T_R \leq 7$ days	$T_d \geq 3$ month
7 days $< T_R \leq 30$ days	$T_d \geq 1$ year
30 $< T_R \leq 180$ days	$T_d \geq 10$ years
$T_R > 180$ days	$T_d \geq 100$ years

The operation length is defined by an operation reference period, T_R given by Equation 2.1, [1].

$$T_R = T_{POP} + T_C \tag{2.1}$$

The planned operation period (T_{POP}) should normally be based on a detailed schedule for the operation. Where the time estimated for each task in the schedule should be based on reasonable conservative assessment. Frequently experienced time delaying incidents should be included in the estimate.

Contingency time, T_C shall be added to cover general uncertainty in the planned operation time, and possible contingency situations that will require additional

time. The planned operation period start point for a weather restricted operation shall normally be defined from the last weather forecast as shown in Figure 2.10.

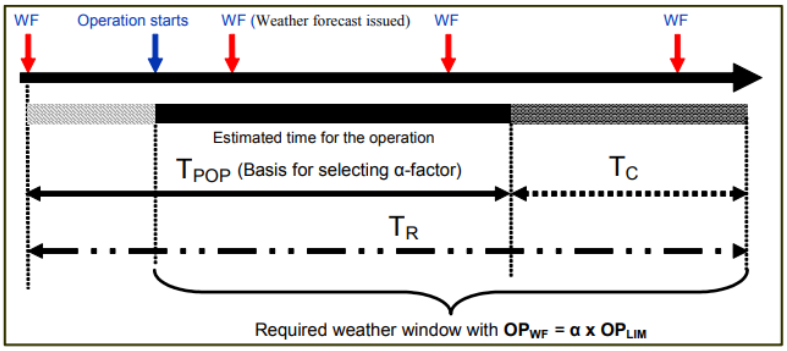

Figure 2.10: Operation periods, [1]

2.3.1 Weather windows and operability

Weather windows are periods of time which are sufficient in length to safely carry out the planned marine operation, and with weather forecasted environmental conditions below the operational criterion. Figure 2.11 shows the significant wave height over time compered to the operational limit. In order to determine the amount of time during a chosen time frame it is possible to perform the operation Equation 2.2 can be used, assuming significant wave height H_S, is the limiting parameter. If another weather parameter is the limiting factor the approach is the same. The probability that the significant wave height is lower than the operational limit is estimated from hindcasting based on observed data for the location, using cumulative probability distribution. Then the probability for sufficient length of calms can be estimated using Equation 2.4 where β and t_c are estimated for a given geographical area and significant wave height. After determining a suitable β t_c can be determined using Equation 2.5. Where A and B are area dependent and can be found by By plotting the cumulative distribution of wave heights vs the average length of calms, and fitting a Weibull distribution. The availability of the operation is then given by Equation 2.6.

$$T_{op} = T_{tot} \cdot P[(H_S \leq OP_{WF}) \cap (\tau_c > T_R)] = Q_{\tau_c}(T_R) \cdot F_{H_S}(OP_{wf}) \cdot T_{tot} \tag{2.2}$$

$$P(H_S \leq OP_{wf}) = F_{H_S}(OP_{wf})) \tag{2.3}$$

$$P(t_c(OP_{wf}) > T_R) = Q_{\tau_c(OP_{wf})}(T_R) = exp(-(\frac{T_R}{t_c})^{\beta}) \tag{2.4}$$

$$t_c = \frac{A \cdot (-ln(F_{H_S}(OP_{wf}))^{-\frac{1}{B}}}{\Gamma(1+\frac{1}{\beta})} \tag{2.5}$$

$$F_{H_S}(OPwf) \cdot Q_{\tau_c(OP_{wf})}(T_R) \tag{2.6}$$

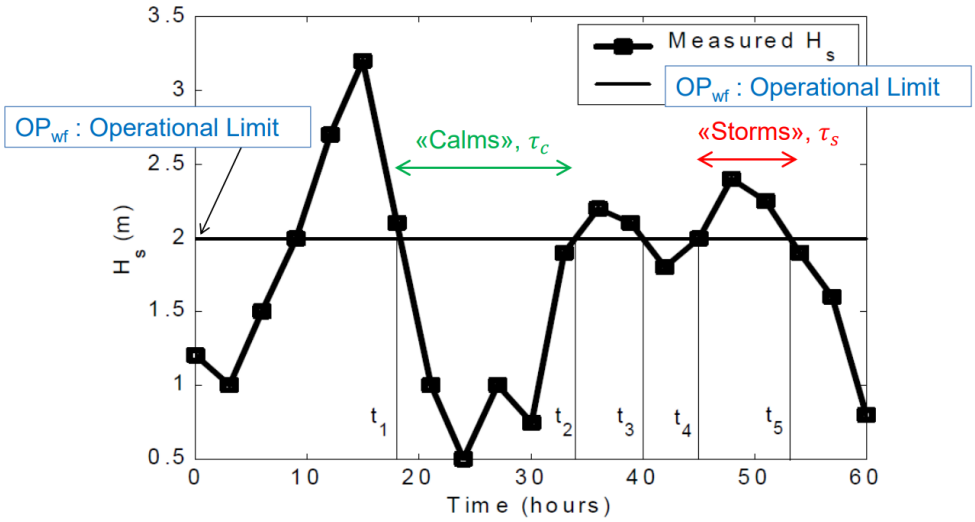

Figure 2.11: Example on on significant wave height as function of time. Linear interpolation between values measured ever 3rd hour, [13]

Chapter 3

Design Methodology

When designing a towing operation the forces acting on the system and subsequent motions needs to be understood. Figure 3.1 shows the forces acting on the system during the operation. It is necessary to determine the required bollard pull of the tug, the required strength of the towing line, required length of the towing line, the effect of propeller race, configuration of the towline, stiffness of the tow line and extreme towline tension among others. Both static and dynamic load effects must be understood.

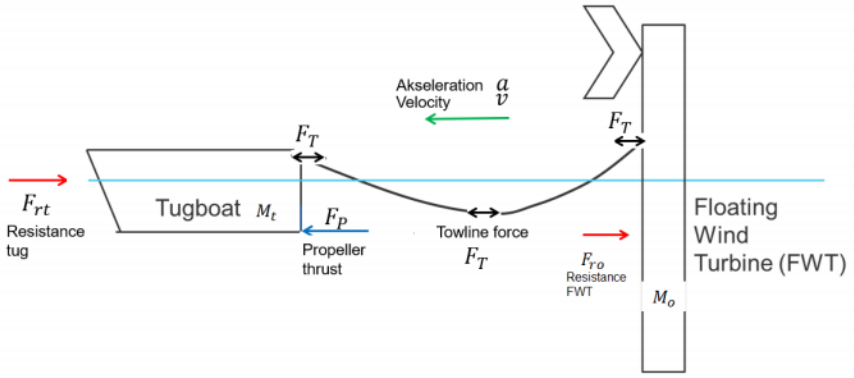

Figure 3.1: Forces acting during tow in head sea,[8]

3.1 Mean towline tension

Static analysis can be used to determine the mean towline tension and the required bollard pull from the tugboat in Figure 3.1 as shown in Equation 3.1. Where the drag resistance for the tug and towed object is calculated using the mean drag resistance from wind, waves and current forces as shown in Equation 3.2. The mean towline tension is equal to the mean resistance on the towed object, and M_t and M_0 is the mass of the tug and FWT respectively.

$$F_P = F_{rt} + F_{ro} + (M_t + M_0) \cdot a \tag{3.1}$$

$$F_r = F_{wi} + F_{wd} + F_{cu} \tag{3.2}$$

The wind and current forces can be calculated using Equation 3.3 and 3.4 for both the tugboat and towed object individually. Using their respective drag coefficients, densities, exposed area and relative velocity.

$$F_{wi} = \frac{1}{2}\rho_a \cdot C_D \cdot Area \cdot V_{rwi}^2 = c_{wi} V_{rwi}^2 \tag{3.3}$$

$$F_{cu} = \frac{1}{2}\rho_a \cdot C_D \cdot Area \cdot V_{rwi}^2 = c_{cu} V_{rc}^2 \tag{3.4}$$

The relative velocity is defined as given in Equation 3.5. Where V_{1x} and V_{1y} is the x and y velocity of object one respectively, and V_{2x} and V_{2y} are the corresponding velocities for the second object in this case current or wind.

$$\vec{V_r} = (V_{1x} - V_{2x})\hat{i} + (V_{1y} - V_{2y})\hat{j} \tag{3.5}$$

The wave drift force can be calculated as shown in Equation 3.6 using the JONSWAP spectrum as shown in Equation 3.7, [14].

$$F_{wd} = 2\int_{\infty} S(\omega)c(\omega)d\omega \tag{3.6}$$

$$S_\omega = 155\frac{H_s^2}{T_1^4\omega^5}exp(\frac{-944}{T_1^4\omega^4})(3.3)^Y \tag{3.7}$$

where
$c(\omega)$ = The mean wave drift force coefficient
H_s = Significant wave height defined as the mean of the one third highest waves.
T_1 = Mean wave period given by Equation 3.8.
and Y is given by Equation 3.10 with σ=0.07 for $\omega \leq 5.24/T_p$ and σ=0.09 for $\omega > 5.24/T_p$, [14].

$$T_1 = 2\pi m_0/m_1 = 0.834T_P \tag{3.8}$$

$$m_k = \int_{\infty} \omega^k S(\omega)d\omega \tag{3.9}$$

$$Y = exp(-(\frac{0.191\omega T_p - 1}{2^{0.5}\sigma})^2) \tag{3.10}$$

The strength requirements of the towing line can be estimated based on the required bollard pull of the vessel. Table 3.1 gives minimum design load for all components in the main towing line. The minimum, certified breaking strength

Table 3.1: Design load of towing line BP: Continuous static bollard pull of the vessel in tonnes. [2]

F_{TD}=3.0 BP	BP $\leq$ 40
F_{TD}=(220-BP)BP/60	40 <BP <100
F_{TD}=2.0 BP	BP $\geq$ 100

(MBL) of the towline shall be equal or grater then the F_{TD} for both main and spare towlines. as well as he emergency towline [2].

The minimum length of the towline for a given bollard pull is given by DNVGL as shown in Equation 3.11 for unrestricted towing and Equation 3.12 for benign water areas [2].

$$L_{min} = 1800BP/F_{TD} \tag{3.11}$$

$$L_{min} = 1200BP/F_{TD} \tag{3.12}$$

3.2 Static towing line configuration

For a towing cable where the towline tension is much larger than the wight of the cable, the horizontal $x(s)$ and vertical $z(x)$ coordinates along the towline can be approximated for by static analysis with the following parametric equations [5].

$$x(s) = (1 + \frac{T_0}{EA})s.\frac{1}{6}(\frac{w}{T_0})^2 s^3 \tag{3.13}$$

$$z(s) = -z_m + \frac{1}{2}\frac{ws^2}{T_0}(1 + \frac{T_0}{EA}) \tag{3.14}$$

where
T_0 = towline tension [N]
E = modulus of elasticity of towline [N/m^2]
A = nominal cross-sectional area of towline [m^2]
w = submerged weight per unit length of towline [N/m]
s = coordinate along the towline (-L/2 < s < L/2) [m]
z_m = sag of towline at centre [m] given by Equation 3.15 [5]
L = length of towline [m]

$$z_m = \frac{L}{8}(\frac{wL}{T_0})(1 + \frac{T_0}{EA}) \tag{3.15}$$

Figure 3.2 shows a typical static geometry of a towline. When towing in shallow water a sufficient clearance between towline and seabed must be ensured by controlling the towline length and tension.

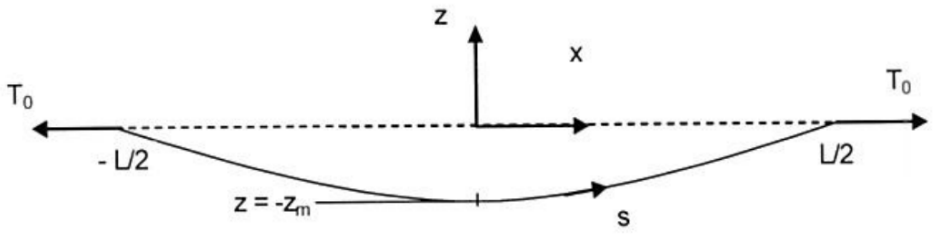

Figure 3.2: Standard geometry of a towing line,[5]

3.3 Effect of Propeller Race

When short towlines are applied the tug propeller may induce flow velocities at the towed structure which increases the towing resistance significantly. If the towed structure is small compared to the transverse dimensions of the propeller race the velocity in the propeller race may be considered as an increased towing velocity when calculating the towing resistance [4].

When the towed structure large compared to the dimensions of the propeller race. The additional towing resistance can be estimated by use of momentum considerations. The thrust of the propeller with diameter D is equal to the axial flux of momentum through the propeller disk as shown in Equation 3.16. When assuming the flow velocity through the disk to be homogenous and denoted U_0.

$$\frac{dM}{dt} = F_p = \rho_w \frac{\pi D^2}{4} U_0^2 \tag{3.16}$$

In an unbounded and ideal fluid the axial component of the flux of momentum will be constant through every cross section behind the propeller. However, if a body is inserted in the propeller race the direction of the flow will be modified and a force will act on the body as a consequence, see Figure 3.3, [4].

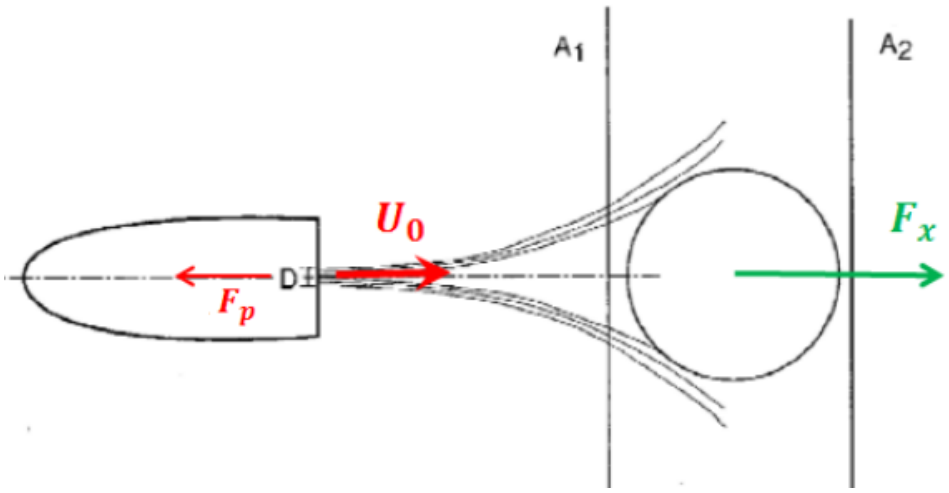

Figure 3.3: Deflection of the propeller race by a towed body,[8]

When considering the axial flux of momentum through the two infinite planes A_1 and A_2. The difference in flux of momentum must represent the axial force on the body:

$$F_x = \frac{dM_{1x}}{dt} - \frac{dM_{2x}}{dt} = \rho_w \int_{A_1} U_x^2 dA - \rho_w \int_{A_2} U_x^2 dA \tag{3.17}$$

This results in two extreme cases. The first there is no change in momentum and hence no net force on the body. Friction due to viscous effects could, however still, give a small force on. If the the propeller race is completely reversed as shown in Figure 3.4. The e force on the towed object is twice the propeller thrust and the total force on the tug and towed structure will F_p-2F_p=-F_p, resulting in the system moving backwards [4].

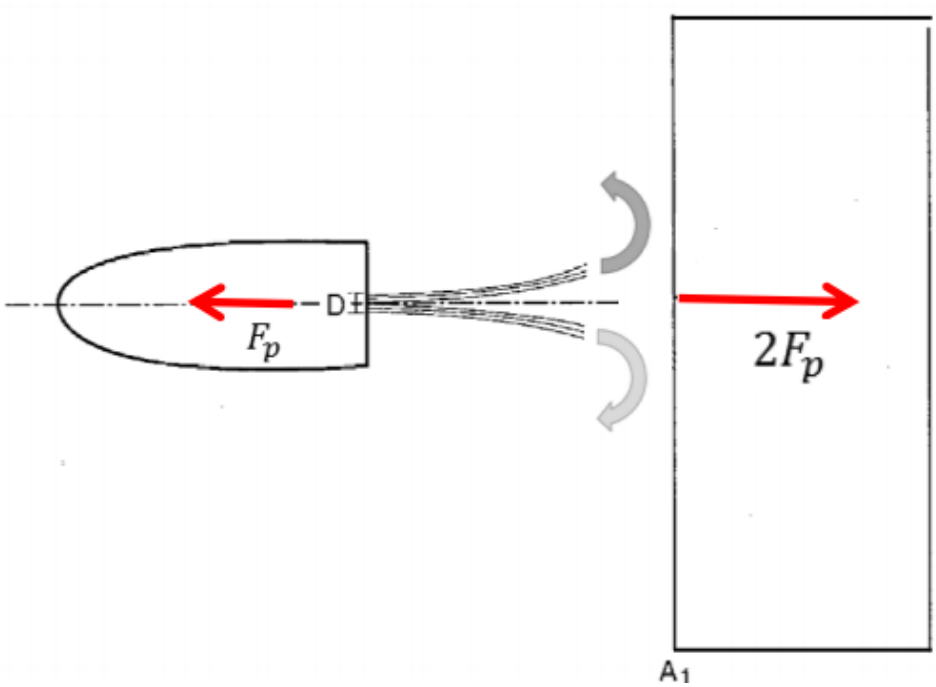

Figure 3.4: Propeller race completely reversed,[8]

For towlines longer than 30 m, the effect of propeller race is taken into account by reducing the available bollard pull by an interaction efficiency factor [2] as shown in Equation 3.18

$$\alpha_{int} = [1 + 0.015 A_{exp_{tow}} / L_{towline}]^{-\eta}[-] \tag{3.18}$$

3.4 Sway/Yaw Stiffness

A bridle is used to improve manoeuvrability and course stability of the towed structure. When the towed structure is rotated an angle α the forces in each of the bridle lines will be different as shown in Figure 3.5. . Assuming each bridle line forms an angle β with the towing line, and the towing force is T_0, the distribution of forces in each bridle line for small rotation angles, is given by the following equations, [5];

$$\frac{T_{b1}}{T_{b0}} = \frac{sin(\beta + \alpha + \gamma)}{sin(2\beta)}(N/N) \tag{3.19}$$

$$\frac{T_{b2}}{T_{b0}} = \frac{sin(\beta + \alpha + \gamma)}{sin(2\beta)}[N/N] \tag{3.20}$$

$$\gamma = \frac{R}{L_{towline}}\alpha[R] \tag{3.21}$$

where
T_{b0} = towing force [N]
T_{b1} = force in port bridle [N]
T_{b2} = force in starboard bridle [N]
R = distance from centre of gravity of towed structure to end of bridle lines [m]
α = angle of rotation of towed structure [rad]
β = angle between each of the bridle lines and the vessel centre line [rad]

For the sett up shown in Figure 3.5 the force in the starboard bridle then becomes zero when:

$$\alpha = \frac{L_{towline}\beta}{L_{towline} + R} \tag{3.22}$$

For rotation angles larger than this, one bridle line goes slack and the other line will take all the load. The moment of the towing force around the rotation centre f the towed structure is given as;

$$M_G = T_0 R(1 + \frac{R}{L})\alpha \tag{3.23}$$

and the rotational stiffness due to the towing force is given by;

$$C_{66} = T_0 R(1 + \frac{R}{L}) \tag{3.24}$$

Hence, the bridle contributes with a substantial increase in the rotational stiffness, improving the directional stability of the tow [5].

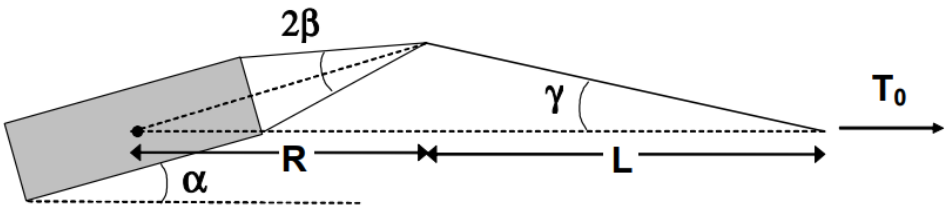

Figure 3.5: Layout of towline and bridle lines,[5]

3.5 Towline stiffness

The towline stiffness can be approximated as to springs in series. Where one spring represents the elastic stiffness due to elastic elongation, and the second spring represents the geometric stiffness due to change of geometry of the the towline. The resulting stiffness in the towing line is given by the equations 3.25, 3.26 and 3.27, [5].

$$k_G = \frac{12T_0^3}{(wL)^2 L} \tag{3.25}$$

$$k_E = \frac{EA}{L} \tag{3.26}$$

$$\frac{1}{k_{tot}} = \frac{1}{k_E} + \frac{1}{k_G} \tag{3.27}$$

3.6 Extreme towline tension

The dynamic tension in the towline can be used as input in some of the static calculations above. For example if ensuring sufficient clearance between towline and seabed the mean towline tension will not give a conservative estimate, and therefore the critical values from the dynamic tension may be required. The extremes for the towline tension are dependent of the relative motions of the towing vessel and the towed object. Large towed objects have small motion responses to the waves relative to the towing vessel, and as a result will have a negligible effect on the towline tension. There are several methods for estimating the extreme towline tension. Two main methods have been used as a part of this master thesis frequency response and time domain analyses. Below the main methods have been described when the motion of the towed object is assumed negligible.

3.6.1 Frequency response

The frequency response method used in this thesis assumes negligible motions on the towed objects, and the effect of the towing line on the dynamic motions of the vessel are negligible. Using the RAOs for the vessel motions at the centre of gravity (COG) the RAOs for the motions at the attachment point of the towing line is determined. This is done using the motion transfer functions shown Equation 3.28, 3.29 and 3.30 on the vessel RAO's. The resulting phases of the motions at the attachment point is then determined using Equation 3.31, 3.32 and 3.33.

$$\begin{aligned}\eta_{1_{AP}}(x,y,z) = \Big\{ &(\eta_{1_{COG}} \cdot cos(\theta_{1_{COG}}) + \eta_{5_{COG}} \cdot z \cdot cos(\theta_{5_{COG}}) - \\ &\eta_{6_{COG}} \cdot y \cdot cos(\theta_{6_{COG}}))^2 + (\eta_{1_{COG}} \cdot sin(\theta_{1_{COG}}) + \\ &\eta_{5_{COG}} \cdot z \cdot sin(\theta_{5_{COG}}) - \eta_{6_{COG}} \cdot y \cdot sin(\theta_{6_{COG}}))^2 \Big\}^{1/2}\end{aligned} \tag{3.28}$$

$$\begin{aligned}\eta_{2_{AP}}(x,y,z) = \Big\{ &(\eta_{2_{COG}} \cdot cos(\theta_{2_{COG}}) + \eta_{4_{COG}} \cdot z \cdot cos(\theta_{4_{COG}}) - \\ &\eta_{6_{COG}} \cdot x \cdot cos(\theta_{6_{COG}}))^2 + (\eta_{2_{COG}} \cdot sin(\theta_{2_{COG}}) + \\ &\eta_{4_{COG}} \cdot z \cdot sin(\theta_{4_{COG}}) - \eta_{6_{COG}} \cdot x \cdot sin(\theta_{6_{COG}}))^2 \Big\}^{1/2}\end{aligned} \tag{3.29}$$

$$\eta_{3_{AP}}(x,y,z) = \Big\{(\eta_{3_{COG}} \cdot cos(\theta_{3_{COG}}) + \eta_{4_{COG}} \cdot y \cdot cos(\theta_{4_{COG}}) - \eta_{5_{COG}} \cdot x \cdot cos(\theta_{5_{COG}}))^2 + (\eta_{3_{COG}} \cdot sin(\theta_{3_{COG}}) + \eta_{4_{COG}} \cdot y \cdot sin(\theta_{4_{COG}}) - \eta_{5_{COG}} \cdot x \cdot sin(\theta_{5_{COG}}))^2\Big\}^{1/2} \tag{3.30}$$

$$\theta_{1_{AP}}(x,y,z) = arcsin = \frac{(\eta_{1_{COG}} \cdot sin(\theta_{1_{COG}}) + \eta_{5_{COG}} \cdot z \cdot sin(\theta_{5_{COG}}) - \eta_{6_{COG}} \cdot y \cdot sin(\theta_{6_{COG}}))}{(\eta_{1_{COG}} \cdot cos(\theta_{1_{COG}}) + \eta_{5_{COG}} \cdot z \cdot cos(\theta_{5_{COG}}) - \eta_{6_{COG}} \cdot y \cdot cos(\theta_{6_{COG}}))} \tag{3.31}$$

$$\theta_{2_{AP}}(x,y,z) = arcsin = \frac{(\eta_{2_{COG}} \cdot sin(\theta_{2_{COG}}) + \eta_{4_{COG}} \cdot z \cdot sin(\theta_{4_{COG}}) - \eta_{6_{COG}} \cdot x \cdot sin(\theta_{6_{COG}}))}{(\eta_{3_{COG}} \cdot cos(\theta_{3_{COG}}) + \eta_{4_{COG}} \cdot y \cdot cos(\theta_{4_{COG}}) - \eta_{6_{COG}} \cdot x \cdot cos(\theta_{6_{COG}}))} \tag{3.32}$$

$$\theta_{3_{AP}}(x,y,z) = arcsin = \frac{(\eta_{3_{COG}} \cdot sin(\theta_{3_{COG}}) + \eta_{4_{COG}} \cdot y \cdot sin(\theta_{4_{COG}}) - \eta_{5_{COG}} \cdot x \cdot sin(\theta_{5_{COG}}))}{(\eta_{3_{COG}} \cdot cos(\theta_{3_{COG}}) + \eta_{4_{COG}} \cdot y \cdot cos(\theta_{4_{COG}}) - \eta_{5_{COG}} \cdot x \cdot cos(\theta_{5_{COG}}))} \tag{3.33}$$

where,

x = The x position of the attachment point in the local coordinate system
y = The y position of the attachment point in the local coordinate system
z = The z position of the attachment point in the local coordinate system
$\eta_{1_{AP}}$ = Surge motion at attachment point
$\eta_{2_{AP}}$ = Sway motion at attachment point
$\eta_{3_{AP}}$ = Heave motion at attachment point
$\theta_{1_{AP}}$ = Phase of the surge motion at attachment point
$\theta_{2_{AP}}$ = Phase of the sway motion at attachment point
$\theta_{3_{AP}}$ = Phase of the heave motion at attachment point
$\eta_{1_{COG}}$ = Surge motion at centre of gravity
$\eta_{2_{COG}}$ = Sway motion at centre of gravity
$\eta_{3_{COG}}$ = Heave motion at centre of gravity
$\eta_{4_{COG}}$ = Roll motion at centre of gravity
$\eta_{5_{COG}}$ = Pitch motion at centre of gravity
$\eta_{6_{COG}}$ = Yaw motion at centre of gravity
$\theta_{1_{COG}}$ = Phase of the surge motion at centre of gravity
$\theta_{2_{COG}}$ = Phase of the sway motion at centre of gravity
$\theta_{3_{COG}}$ = Phase of the heave motion at centre of gravity
$\theta_{4_{COG}}$ = Phase of the roll motion at centre of gravity
$\theta_{5_{COG}}$ = Phase of the pitch motion at centre of gravity
$\theta_{6_{COG}}$ = Phase of the yaw motion at centre of gravity

In order to find the motion response along the line the angle of approach is required and can be determined using Equation 3.34. Using Equation 3.35 the RAO for motion along the towing line can be determined.

$$\phi = arctan(\frac{w \cdot \frac{L}{2}}{\overline{T}}) \tag{3.34}$$

$$\eta_\phi(x,y,z) = \Big\{((\eta_{1_{AP}} \cdot cos(\phi)) \cdot cos(\theta_{1_{AP}}) - ((\eta_{3_{AP}} \cdot cos(\frac{\pi}{2} - \phi) \cdot cos(\theta_{3_{AP}})))^2 + ((\eta_{1_{AP}} \cdot cos(\phi)) \cdot sin(\theta_{1_{AP}}) - ((\eta_{3_{AP}} \cdot cos(\frac{\pi}{2} - \phi) \cdot sin(\theta_{3_{AP}})))^2 \Big\}^{1/2} \tag{3.35}$$

where,
$\overline{T}$ = Mean tension in towing line
w_0 = Weight per unit length in unstretched condition
η_ϕ = Motion along towline

The resulting tension in the towline from the vessel motion along the line can be found using hooke's law, where the spring constant is set as the towline stiffness. The RAO between the tension in the towing line and the wave can then be determined using Equation 3.36.

$$\frac{T_0}{\zeta_a} = \frac{\eta_\phi}{\zeta_a} \cdot \frac{T_0}{\eta_\phi} \tag{3.36}$$

Where,
ζ_a = Wave amplitude

When determining the towline stiffness the towline can be modelled as two spring in series and a damper as seen in Figure 3.6. This model builds on the approximation of towline stiffness in Equation 3.27, by adding the damper to simulate transverse drag forces on the line. The resulting stiffness can be conservatively estimated by assuming drag locking. Drag locking is when the vertical motion of the towline is restricted due to drag forces. This results in the geometric elasticity to be "locked" and as a result only elastic stiffness is used.

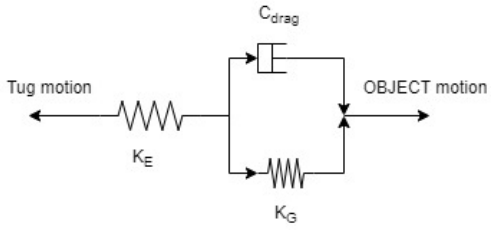

Figure 3.6: Dynamic model for a simplified dynamic analysis of the towing line

Where,
C_{drag} = Linearized damping coefficient due to drag on towline

In order to determine the actual stiffness the damping coefficient C_{drag} must be estimated. Using the governing equations for the static towing line configurations

and making the following simplifications. Removing the elasticity and assuming T_0 is much larger than w. Results in the simplified equations shown in Equation 3.37, 3.38 and 3.39

$$x(s) \approx s \tag{3.37}$$

$$z(s) \approx z(x) \approx -z_m + \frac{1}{2}\frac{wx^2}{T_0} \approx \frac{w}{8T_0} \cdot (4x^2 - L^2) \tag{3.38}$$

$$Z_m \approx \frac{wL^2}{8T_0} \tag{3.39}$$

Figure 3.7 shows a model of the towing line, where the object motions have been assumed negligible. The amplitude of dynamic tension T_a is assumed to be the same over the spring K_E, as over the total over K_G and C_{drag} as shown in Equation 3.40. The variable u_a represents the "amplitude" of the towline causing geometric change and transverse drag resistance. Solving Equation 3.40 for u_a results in Equation 3.42. The amplitude of vessel motion x_a and dynamic tension is for a given frequency

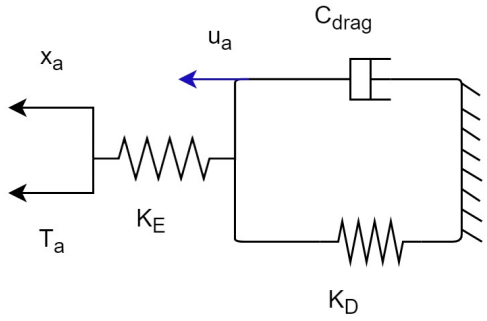

Figure 3.7: Model of towline stiffness for calculation of linearized damping coefficient

$$T_a = K_E \cdot (x_a - u_a) = u_a \cdot \sqrt{(C_{drag}\omega)^2 + K_G^2} \tag{3.40}$$

$$K_E \cdot x_a = u_a(K_E + \sqrt{(C_{drag}\omega)^2 + K_G^2}) \tag{3.41}$$

$$u_a = \frac{K_E}{K_E + \sqrt{(C_{drag}\omega)^2 + K_G^2}} \cdot x_a \tag{3.42}$$

The expression for u_a can then be inserted into Equation 3.40 and solved for T_a divided by x_a resulting in Equation 3.43. This is the linearized transfer function for the tension in the towline for a given amplitude of motion along the line.

$$\frac{T_a}{x_a} = K_E \cdot (1 - \frac{K_E}{K_E + \sqrt{(C_{drag}\omega)^2 + K_G^2}}) \tag{3.43}$$

In order to estimate the equivalent, linearized damping coefficient, C_{drag} half of the line is considered. Imposing a motion amplitude u_x and a velocity amplitude $\dot{u}_x = \omega \cdot u_a$ at the end. This will result in the line moving vertically with an amplitude $z_a(x)$ and a corresponding velocity amplitude $\dot{z_a}(x) = \omega \cdot z_a(x)$ which are functions of x. In order to estimate the drag resistance due to this motion, the drag force of a small element dx along the line is required. This is easily estimated using the transverse velocity of the element dx, which can be determined using Equation 3.44. Equation 3.38 gives Equation 3.45 and Equation 3.46 is given by hooks law assuming no elasticity and damping in the towing line. The resulting transverse motion and velocity is given by Equation 3.47

$$\frac{dz(x)}{du} = \frac{dz(x)}{dT_0} \cdot \frac{dT_0}{du} \tag{3.44}$$

$$\frac{dz(x)}{dT_0} = \frac{w}{8T_0^2} \cdot (L^2 - 4x^2) \tag{3.45}$$

$$\frac{dT_0}{du} = K_G \tag{3.46}$$

$$\begin{aligned} z_a(x) &= \frac{w}{8T_0^2} \cdot (L^2 - 4x^2) \cdot K_G \cdot u_a \\ \dot{z}_a(x) &= \frac{w}{8T_0^2} \cdot (L^2 - 4x^2) \cdot K_G \cdot \dot{u}_a \end{aligned} \tag{3.47}$$

The total drag force is then estimated by moment equilibrium around the centre point of the towing line as shown in Equation 3.48. The drag force on the line element dx can be calculated using Equation 3.49. Inserting the expressions into Equation 3.48 results in Equation 3.50, and solving the integral gives Equation 3.51

$$\sum M_p = 0 \rightarrow T_d \cdot z_m = \int_0^{L/2} dF(x) \cdot x \cdot dx \tag{3.48}$$

$$dF(x) = \frac{1}{2}\rho_w C_d \cdot D_{line} \cdot \dot{z}_a^2(x) = K_D \cdot \dot{z}_a^2(x) \tag{3.49}$$

$$T_D \cdot \frac{wL^2}{8T_0} = \int_0^{L/2} K_D \cdot [\frac{w}{8T_0^2} \cdot (L^2 - 4x^2) \cdot K_G]^2 \cdot \dot{u}_a^2 \cdot x \cdot dx \tag{3.50}$$

$$T_D = \frac{3}{4} K_D \cdot \frac{T_0^3}{w^3 \cdot L^2} \cdot \dot{u}_a^2 \tag{3.51}$$

where,
D_{line} = Diameter of the towing line
T_D = Tension in towing line due to drag

Equation 3.51 needs to be linearized this is done using stochastic linearization of $\dot{u}_a^2$ resulting in Equation 3.52, where the tension due to drag is set equal to C_{drag} times $\dot{u}_a$ as it is modelled by the damper.

$$T_D = \frac{3}{4} K_D \cdot \frac{T_0^3}{w^3 \cdot L^2} \cdot \sqrt{\frac{8}{\pi}} \cdot \sigma_{\dot{u}} \cdot \dot{u}_a = C_{drag} \cdot \dot{u}_a \tag{3.52}$$

$$C_{drag} = \frac{3}{4} K_D \cdot \frac{T_0^3}{w^3 \cdot L^2} \cdot \sqrt{\frac{8}{\pi}} \cdot \sigma_{\dot{u}} \tag{3.53}$$

Equation 3.53 gives that in order to determine C_{drag} the standard deviation of the velocity $\dot{u}$ is required. From Equation 3.42 the transfer function from the vessel motion is known, assuming no drag results in Equation 3.54.

$$\begin{aligned} \sigma_u &= \frac{K_E}{K_E + \sqrt{(C_{drag}\omega)^2 + K_G^2}} \cdot \sigma_x \\ \sigma_{\dot{u}} &= \frac{K_E}{K_E + \sqrt{(C_{drag}\omega)^2 + K_G^2}} \cdot \sigma_{\dot{u}} \end{aligned} \tag{3.54}$$

Where,
σ_x = Standard deviation of vessel motion
$\sigma_{\dot{u}}$ = Standard deviation of vessel velocity

The standard deviation of vessel motion and velocity is determined from the frequency spectrum of vessel motion, x and velocity, $\dot{x}$. as shown in Equation 3.55

$$\begin{aligned} \sigma_x &= \sqrt{\int S_x(\omega) dw} \\ \sigma_{\dot{x}} &= \sqrt{\int S_{\dot{x}}(\omega) dw} \end{aligned} \tag{3.55}$$

In order to estimate $\sigma_{\dot{u}}$ an iteration process is used initialised by assuming no drag resistance, then calculate C_{drag} using Equation 3.53. With the calculated drag generate an updated geometric "stiffness" using Equation 3.56. With the updated "stiffness" calculate amplification factor (f) of geometric "stiffness" using Equation 3.57. After calculating the amplification factor, calculate a new temporary $K_{G_{temp}}$=K_G·f. Using the new temporary stiffness calculate a new $\sigma_{\dot{u}}$ and use this and the temporary stiffness to calculate a updated C_e. Stop the iteration when both C_e and $\sigma_{\dot{u}}$ have converged.

$$K_g' = \sqrt{(C_e \sigma_{\dot{u}})^2 + (K_G \sigma_u)^2} \tag{3.56}$$

$$f = \frac{K'_G}{K_G \cdot \sigma_{u,i}} \tag{3.57}$$

With the converged C_e the linearized transfer function can be quantified using Equation 3.43. The RAO between dynamic towline tension and wave motion, ζ can then be found using Equation 3.36 when using $x_a = \eta_\phi$ as shown in Equation 3.58. The frequncy spectrum of towing line tenison can now be found using Equation 3.59.

$$\frac{T_D}{\zeta_a} = \frac{\eta_\phi}{\zeta_a} \cdot \frac{T_D}{\eta_\phi} = \frac{x_a}{\zeta_a} \cdot \frac{T_D}{x_a} = H(\omega) \tag{3.58}$$

$$S_T(\omega) = |H(\omega)|^2 \cdot S(\omega) \tag{3.59}$$

The n'th moments of a spectrum is defined as shown in Equation 3.60, [15]. The standard deviation can be calculated from the spectral moments as shown in Equation 3.61. The most probable maximum (MPM) response for a given number of periods, N can be determined using Equation 3.62, where 'log' is the natural logarithm [14]. The most probable maximum tension can with this be found for the spectrum $S_T(\omega)$, the corresponding maximum towline tension is equal to the sum of the dynamic tension and the mean tension as show in Equation 3.63.

$$m_n = \int_0^\infty \omega^n S(\omega) d\omega \tag{3.60}$$

$$\sigma = \sqrt{m_0} \tag{3.61}$$

$$MPM = \sigma_{T_D} \cdot \sqrt{2 \cdot log(N)} \tag{3.62}$$

$$T_{tot_{MPM}} = \overline{T} + T_{D_{MPM}} \tag{3.63}$$

3.6.2 Time domain

Time domain analysis solves the equation of motion as shown in Equation 3.64. SIMO have two separate approaches that can be used to solve the equation, separation of motion and total motion. The total motion can be coupled with a finite element analysis of the towline in RIFLEX, while the separation of motion can be combined with a simplified dynamic analysis in SIMO. Alternatively both approaches can be combined with a quasi-static towline model in SIMO, or the resulting motions can be exported and and used as end motions in RIFLEX.

$$\begin{aligned}&(\boldsymbol{m} + \boldsymbol{A}(\omega)) \cdot \ddot{\vec{\eta}} + \boldsymbol{C}(\omega) \cdot \dot{\vec{\eta}} + \boldsymbol{D}_l \cdot \dot{\vec{\eta}} + \boldsymbol{D}_q \dot{\vec{\eta}} |\dot{\vec{\eta}}| \\ &+ \boldsymbol{K}(x) \cdot \vec{\eta} = \vec{q}_{cu}(t) + \vec{q}_{wi}(t) + \vec{q}^1_{wa}(t) + \vec{q}^2_{wa}(t) + \vec{q}_{ext}\end{aligned} \tag{3.64}$$

Where,
$\boldsymbol{M}$ = Body mass matrix
$\boldsymbol{A}(\omega)$ = Frequency-dependent added mass matrix
$\boldsymbol{C}(\omega)$ = Frequency-dependent potential damping matrix
$\boldsymbol{D}_{\mathrm{l}}$ = Linear damping matrix
$\boldsymbol{D}_{\mathrm{q}}$ = Quadratic damping matrix
$\boldsymbol{K}(\eta)$ = Hydrostatic and towline stiffness matrix
$\vec{\eta}$ = Position vector
$\dot{\vec{\eta}}$ = Velocity vector
$\ddot{\vec{\eta}}$ = Acceleration vector
$\vec{q}_{cu}(t)$ = Current drag force vector
$\vec{q}_{wi}(t)$ = Wind drag force vector
$\vec{q}^{1}_{wa}(t)$ = First order wave excitation force vector
$\vec{q}^{2}_{wa}(t)$ = Second order wave excitation force vector
$\vec{q}_{ext}$ = Sum of any other force vectors (wave drift damping, specified forces and forces from station-keeping and coupling elements, etc.)

The current and wind drag forces expressed in Equation 3.3 and 3.4 gets a time dependent relative velocity due to wind gust and the low frequency vessel responses. Equation 3.65 shows an approximation of the wind force assuming mean wind velocity significantly larger than gust and vessel response velocity. Assuming the current velocity also significantly larger than vessel response velocity the current forces can be approximated as shown in Equation 3.66. Both equation shows a low frequency linear damping term due to the changing relative velocities due to vessel response. The mean velocities shown are the relative velocities assuming constant vessel velocity.

$$q_{wi}(t) = c_{wi} \cdot ((\overline{U} + u(t)) - \dot{\eta})^2 \approx c_{wi} \cdot \overline{U}^2 + c_{wi}\overline{U} \cdot u(t) - c_{wi}\overline{U} \cdot \dot{\eta} \tag{3.65}$$

$$q_{cu}(t) = c_{cu} \cdot |\overline{V} - \dot{\eta}| \cdot (\overline{V} - \dot{\eta}) \approx c_{cu} \cdot \overline{V}^2 - c_{cu}\overline{V} \cdot \dot{\eta} \tag{3.66}$$

Where,
$\overline{U}$ = Mean wind velocity
u(t) = Dynamic wind gust velocity
$\overline{V}$ = Mean current velocity

3.6.3 Total motion

With the total motion approach x is solved by numerical integration in time domain using retardation function h(t), due to the frequency dependent added mass and potential damping [16]. The frequency dependent added mass and potential damping can be expressed as shown in Equation 3.67. The equation of motion can then be written as shown in Equation 3.68, where $\mathrm{h}(\tau)$ is shown in Equation 3.69

$$A(\omega) = A_\infty + a(\omega) \quad C(\omega) = C_\infty + c(\omega) \tag{3.67}$$

where
$A_\infty = A(\omega = \infty)$
$C_\infty = C(\omega = \infty) \equiv 0$

$$\begin{aligned}&(\boldsymbol{m} + \boldsymbol{A}_\infty) \cdot \ddot{\vec{\eta}} + \boldsymbol{D}_l \cdot \dot{\vec{\eta}} + \boldsymbol{D_q} \dot{\vec{\eta}} |\dot{\vec{\eta}}| + \boldsymbol{K}(x) \cdot \vec{\eta} + \\ &\int_0^t h(t-\tau) \cdot \dot{\vec{\eta}} = \vec{q}_{cu} + \vec{q}_{wi}(t) + \vec{q}^1_{wa}(t) + \vec{q}^2_{wa}(t) + \vec{q}_{ext}\end{aligned} \tag{3.68}$$

$$h(\tau) = -\frac{2}{\pi} \int_0^\infty \omega a(\omega) sin(\omega\tau) d\omega = \frac{2}{\pi} \int_0^\infty \omega c(\omega) cos(\omega\tau) d\omega \tag{3.69}$$

3.6.4 Separation of motion

When using the separation of motion the motions are separated in a high frequency part and a low frequency part. The high frequency motions are solved in the frequency domain, which require the motions to be linear responses to waves. This means that $\mathbf{D}_\mathrm{q}$, the quadratic damping, is set to be zero and **K** constant. Equation 3.70 shows equation of motion for high frequency motion, where $\mathrm{H}^1(\omega)$ is the first order transfer function between excitation force and wave elevation and $\mathbf{X}_\mathrm{hf}(\omega)$ is the first order transfer function between motion and wave elevation. After solving in the frequency domain inverse fast Fourier transform is used in order to get back to the time domain.

$$\begin{aligned}&(\boldsymbol{m} + \boldsymbol{A}(\omega)) \cdot \ddot{\vec{\eta}}_{hf} + (\boldsymbol{C}(\omega) + \boldsymbol{D}_l) \cdot \dot{\vec{\eta}}_{hf} + \boldsymbol{K} \cdot \vec{\eta}_{hf} = q^1_{hf}(\omega) \rightarrow \\ &\boldsymbol{X}_{hf}(\omega) = (-\omega^2(\boldsymbol{m} + \boldsymbol{A}(\omega)) + i\omega(\boldsymbol{C}(\omega) + \boldsymbol{D}_l) + K)^{-1} \cdot H^1(\omega) \cdot \zeta(\omega)\end{aligned} \tag{3.70}$$

The low frequency motions is then solved with the same realisation for the wave elevation as used for the high frequency motion as shown in Equation 3.71

$$(\boldsymbol{m} + \boldsymbol{A}(\omega = 0)) \cdot \ddot{\vec{\eta}}_{lf} + \boldsymbol{D}_l \cdot \dot{\vec{\eta}}_{lf} + \boldsymbol{D}_q \cdot \dot{\vec{\eta}} |\dot{\vec{\eta}}| + \boldsymbol{K} \cdot \vec{\eta}_{lf} = q_{cu} + q_{wi}(t) + q^2_{lf}(t) \tag{3.71}$$

The total motion is then given as the sum of low and high frequency motions.

3.6.5 Distribution

The wind and wave forces are rarely known exactly and are more likely to be expressed as spectrums. Due to this the time domain simulation can give different responses depending on the wave and wind forces generated. With regard extreme tension this difference can be quite significant in certain conditions. In

order to account for this the analysis can be performed for several wind and wave seeds. Assuming the surface and wave elevation is Gaussian distributed the wave response will be Rayleigh distributed. This will result in the extreme responses being Gumbel distributed. Equation 3.72 show the Gumbel distribution, where the statistical estimation uncertainty depends on the number of seeds and the quality of the asymptotic fit depends on the total length of the estimation.

$$F_y(y) = e^{-e^{-\hat{\alpha}(y-\hat{u})}}, \quad \hat{\alpha} = \frac{c_1}{\hat{s}_y}, \quad \hat{u} = \hat{\mu}_y - \frac{c_1}{c_2}\hat{s}_y \tag{3.72}$$

Where,
$\hat{\mu}_y$ = Average value of extremes
$\hat{s}_y$ = Standard deviation of extremes
c_1 and c_2 = Gumbel estimators dependent on number of seeds

Chapter 4

Hywind Tampen

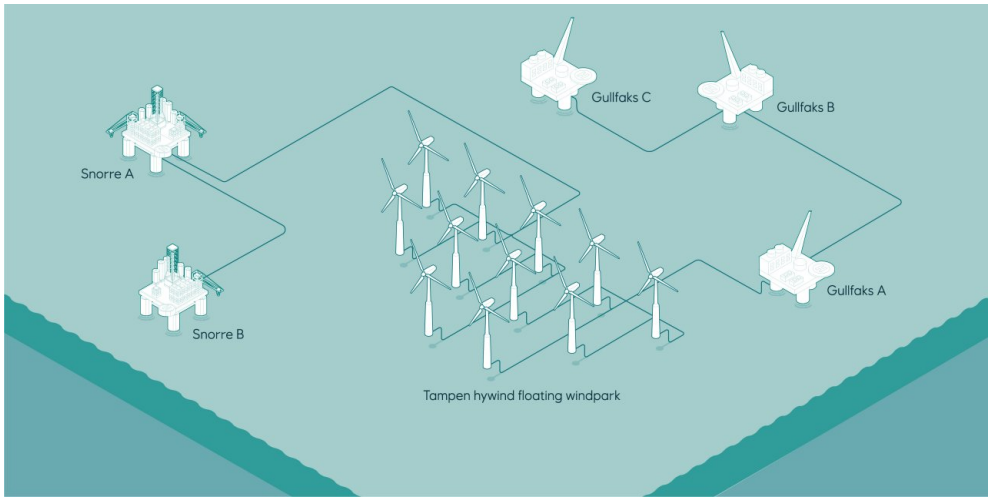

Figure 4.1: Hywind Tampen layout illustration, Equinor

Hywind Tampen is the world's first floating offshore wind farm supplying renewable power to offshore oil and gas installations. Consisting of eleven units with a total capacity of 88 MW. Located approximately 140 km off the Norwegian coast, with a water depth between 260 and 300 metres. The turbines are installed on floating concrete structures wit a shared anchoring system. It will cause significant reduction in CO2 emissions, estimated at 200 000 tonnes per year [17].

The Hywind Tampen FWTs fabrication has four main phases. The first phase consists of slipforming the lower part of the substructure in dry dock at Aker Solution's yard at Stord. The lower parts are then towed to the deep water site at Dommersnes. This is a towing distance of approximately 15Nm, with an estimated towing speed of 2 knots results in a estimated tow time of 7.5 hours.

Where the second phase begins. This phase consists of slipforming the remainder of the substructures. During the slipforming the substructures are floating, which complicates the construction. In order to reduce the motion of the

structures they are attached to barges to crate one large floating structure. This also reduces the rate at which the depth changes when poring concrete as the total mass is larger. The third phase consists of towing from Dommersnes to the main assembly site at Gulen. This is a towing distance of approximately 111Nm, with an estimated towing speed of 2 knots results in a estimated tow time of 55.5 hours.

The fourth phase consists of substructure/tower assembly and commissioning at main commissioning at Wergeland base Gulen. A land based ring crane is used for the crane operations during assembly as show in Figure 4.2. The complete turbine is then towed out to the Tampen field, where the turbine is hooked up to the pre-installed mooring and support system. It is a approximately 130Nm between Gulen and the Tampen field with an estimated towing speed of 2 knots this results in a estimated tow time of 65 hours. The time estimates above does not include a contingency factor. The actual operation times will there for be larger.

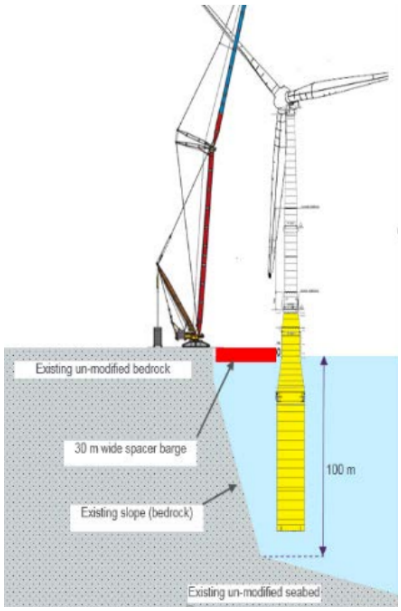

Figure 4.2: Installation with land based crane, Equinor

The towing operation from Gulen to the Tampen Field has been analysed in more detail, with regards to towline tension. For this analyseis the operatin has been planed as a weather unrestricted operation during June, using a single tug-boat with a bollard pull of 500 tonnes.

4.1 Tugboat

In order to analyse the tow from Gulen a model of the tugboat is required. The tugboat was modelled based on vessel data provided by supervisor Kjell Larsen and data from the website "Skipsrevyen.no" ,[18] for the tug "Normand Ferking".

Table 4.1: Vessel data for "Normand Ferking"

LOA [m]	Width [m]	Draft[m]	Δ [tonnes]	T_{η_3} [s]	T_{η_4} [s]	T_{η_5} [s]
99.35	22.00	8	7941	7	14.5	6

The drag coefficients for the tugboat in head wind and current for the surge direction is shown in Table 4.2. The drag coefficients are zero in the other directions for head wind and current and therefor not presented. Figure 4.4, 4.5 and 4.3 shows the surge, heave and pitch RAOs for the tugboat at COG in head sea. In head sea the roll sway and yaw RAO of the tug are zero and there for not presented. The resulting heave motion RAO at the aft of the tug is shown in Figure 4.6. The corresponding wave drift coefficients are shown in Figure 4.7.

Table 4.2: Drag coefficient for tugboat in wind and current for head wind and current

Coefficient	Surge direction
c_{wi}	-0.17573 $[\frac{kNs^2}{m^2}]$
c_{cu}	-27.823 $[\frac{kNs^2}{m^2}]$

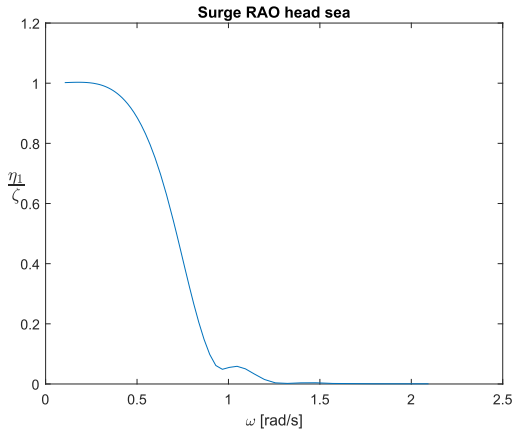

Figure 4.3: Tugboat surge RAO for head sea.

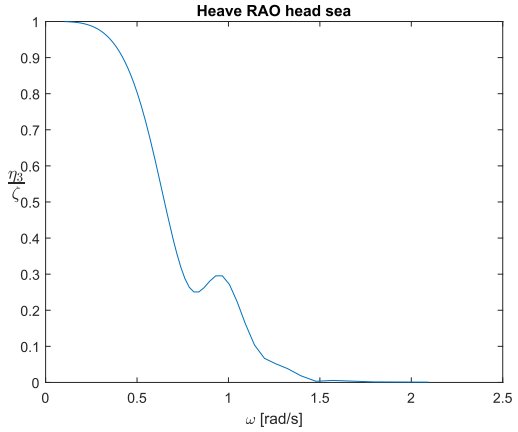

Figure 4.4: Tugboat heave RAO for head sea.

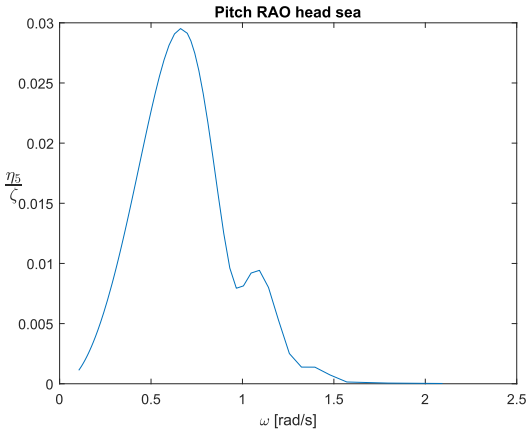

Figure 4.5: Tugboat pitch RAO for head sea.

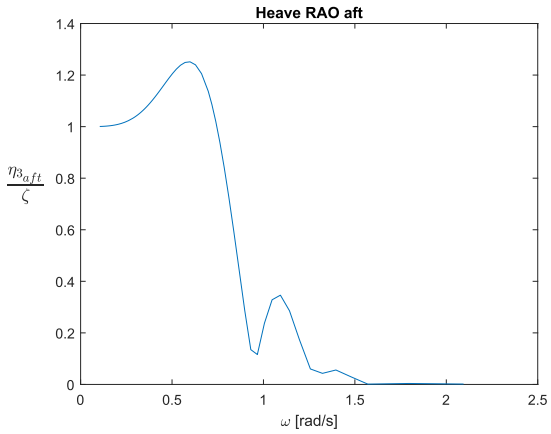

Figure 4.6: Total force on the vessels for H_s=3 [m]

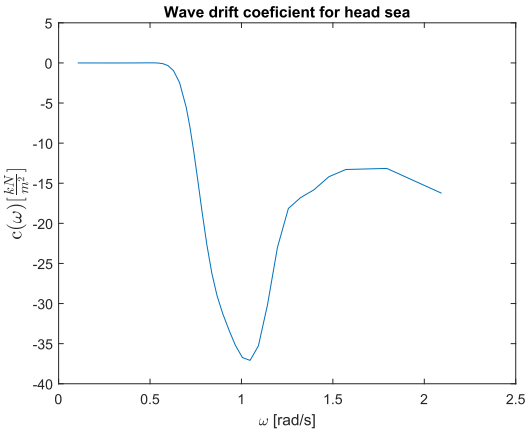

Figure 4.7: Tugboat wave drift coefficients for head sea.

4.2 Hywind Tampen FWT

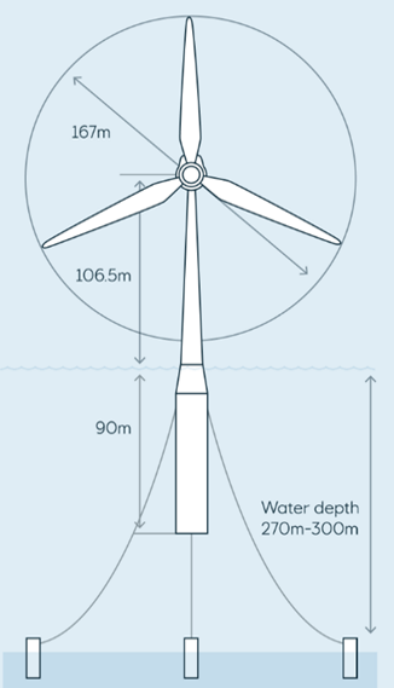

Figure 4.8: Illustration of the Hywind Tampen Floating wind turbine, from Equinor

In order to analyse the forces on the turbine a simplified model was made. Figure 4.8 shows a illustration of the model including some main characteristic dimensions. For the simplified model the FWT was modelled as a two cylinders with a constant diameter. One below the water line with a diameter D_{wet}=18.3 m, and one above the water line with a diameter D_{dry}=8.83 m. Both cylinders were modelled with a drag coefficient C_D=1, chosen from Sea loads on ships and offshore structures figure 6.3, [14]. The blades was modelled as a scaled down version of the turbine used by P.H. Bastiaannssen, [19]. Turbine diameter was used at the basis for the scaling resulting in a scaling factor of 0.78. This assumes the ratio between chord lengths are the same as the blade length ratio. In order to determine the effect of the blade angle, 0 and 90 degree pitch angles relative to the wind were used. The resulting drag coefficients for the blades are shown in Figure 4.9.

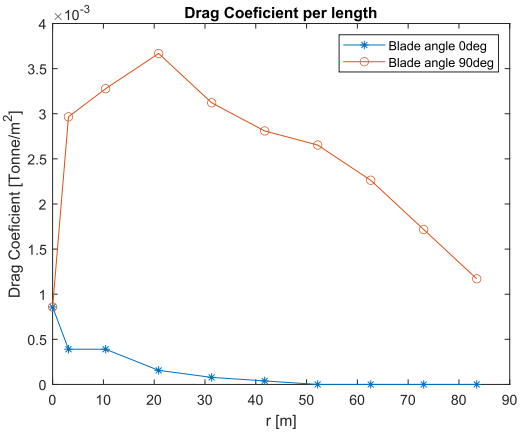

Figure 4.9: Drag coefficient over the length of the blade for varying pitch angles.

The wave drift coefficients c(ω) was estimated from the mean wave load component in regular incident waves divided by the wave amplitude squared. The mean wave load was estimated from Sea loads on ships and offshore structures figure 5.22, [14] assuming a unit wave. The resulting coefficients are shown in Table 4.3 and Figure 4.10.

Table 4.3: Drift coefficient waves on FWT.

ω [1/s]	c(ω) [N] 10^4
0.0011	0
0.1072	0
0.2144	-1.288
0.3216	-2.622
0.4289	-3.956
0.5361	-6.440
0.6422	-11.869
0.7505	-16.561
0.8577	-22.357
0.9649	-27.602
1.0721	-32.846
1.1793	-38.090
1.2866	-43.335

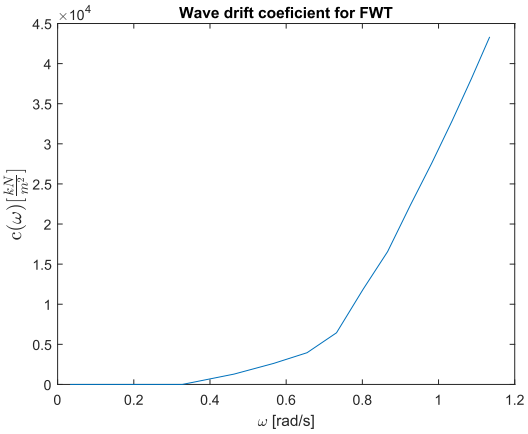

Figure 4.10: FWT wave drift coefficients

4.3 Weather

The weather data used was provided by the supervisor ,[20] and is based on recorded data at the nearby Snorre field. In order to determine the required return periods for the weather the operation reference period i required. Using a contingency factor of 1.5 the 130 Nm tow will result in a reference period larger than 3 days, for a towing speed of 2 knots. But a towing speed of 3 knots will result in a reference period less than 3 days. From Table 2.3 this gives two different return periods 1 month and 3 months. Since the operation is planned for June the 1 month return period will correspond to a annual probability of exceedance of 0.63 for June. While the 3 month return period will correspond to the maximum of the 1 month return periods of May, June and July. The resulting H_s are 6.0 m and 6.1 m for the 1 and 3 month return periods respectively. Due to the small difference, worst case is assumed and the h_s will be sett to 6.1.

The wave period corresponding to the H_s was selected based on recorded periods for given values of H_s at the Snorre Field. From the mean fitted distribution of the recorded values the corresponding peak period was determined, resulting in a period of approximately 12.2 s. The wind speed was chosen as the wind speed with the same probability of non-exceedance as H_s which for a H_s was 0.94%, resulting in a mean wind speed of 17.5 m/s. For the current a probability of non-exceedance at 5 m depth of 99.98% was used resulting in a current speed of 2 knots. A second calmer weather state was also determined using the same method for a H_s of 3 m using the same current speed. Table 4.4 shows both the design and mild weather states.

Table 4.4: Weather data for different weather states

Weather state	H_s [m]	T_p [s]	U_{10} [m/s]	Current speed [Knots]
Design weather	6.1	12.2	17.5	2
Mild weather	3.0	10.0	10.5	2

Chapter 5

Modelling

Several different models have been used to evaluate the towline tension during the tow from Gulen to the Tampen field. The models have a large variation in complexity and required computation time. Below is a short introduction to the different models.

- The first model uses static analysis to estimate the mean towline tension.
- The second model uses the frequency response method to estimate the dynamic tension for different towline models
    - Towline stiffness modelled as pure elastic
    - Geometric stiffness included in the towline stiffness model
    - Linear drag included in the towline stiffness model
- The third model uses separation of motion in the time domain combined with a quasistatic line model
- The Fourth model uses separation of motion in the time domain combined with a simple dynamic line model
- The Fifth model uses total motion in the time domain coupled with a FEA model of the towing line.

Table 5.1 shows which effects are taken into account for the different models as listed above. All the models are modelled with out forward speed. In order to take into account the towing speed relative velocity was used for wind and current. While for the wave loads it was not taken in to account. As such the wave frequency and not the encounter frequency was used. The towing line is modelled as attached to the aft of the tug at the same y and z coordinates as the centre of gravity of the tug.

5.1 Static model Matlab

The first model is used to estimate the mean towline tension and required bollard pull at different towing speeds. Figure 3.1 shows that towline force must be equal to the resistance on the FWT, for the FWT to maintain constant speed. When tow-

Table 5.1: Effects included for different models,*depends on line model

Model	First	Second	Third	Fourth	Fifth
Current forces on tug	mean	mean	included	included	included
Current forces on FWT	mean	mean	mean	mean	mean
Current forces on towing line	not included	linearized*	not included	included	included
Wind forces on tug	mean	mean	included	included	included
Wind forces on FWT	mean	mean	mean	mean	mean
Linear wave forces on tug	not included	included	included	included	included
Linear wave forces on FWT	not included	not included	not included	not included	not included
Quadratic wave forces on tug	mean	mean	included	included	included
Quadratic wave forces on FWT	mean	mean	mean	mean	mean
Towline stiffness force on tug	not included	not included	included	included	included
Towline mass and dragforce on tug	not included	not included	not included	not included	included

ing with a constant average velocity this results in the mean towline tension equal to the mean resistance on the FWT. The required bollard pull is estimated using Equation 3.1 assuming constant speed.

The mean wind, wave and current forces was modelled using Equation 3.3, 3.6 and 3.4 respectively. The velocity in Equation 3.3 is dependent of height above the sea level. This dependency is modelled using Equation 5.1, based on the mean wind speed at 10 m above sea level U_{10} and α=0.12, [21]. For the tugboat U_{10} is used as a uniform wind speed.

$$U_z = U_{10}(\frac{z}{10})^{\alpha} \tag{5.1}$$

The numerical integration of the drift was performed in Matlab. The wind force on the blades of the FWT was modelled the same way as for the tower using the drag coefficient from Figure 4.9. The drag force was calculated for both blade angles.

Based on the required bollard pull the towing speed is determined with regards to the capacity of the tug. The bollard pull is then used to determine the main requirements for the towline dimensions using Table 3.1 and Equation 3.11. While the towline area will be selected as the smallest Spiral Strand steel rope with sufficient MBL based on hardware catalogue provided by supervisor.

5.1.1 Results and discussion

Design weather condition

Figure 5.1 shows the total resistance force on the vessels. with the maximum bollard pull of 500 tonnes the towing speed was selected as 2 knots. It is also observed that the blade angle has a negligible effect.

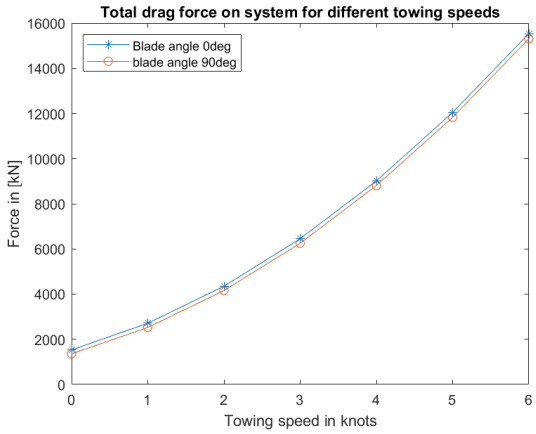

Figure 5.1: Total resistance on the vessels for H_s=6.1 [m]

Figure 5.2 shows that the total resistance on the tug is quite small relative to the total resistance on both vessels. resulting in the total resistance on the FWT being just slightly smaller than the total resistance on the vessels as seen in Figure 5.3.

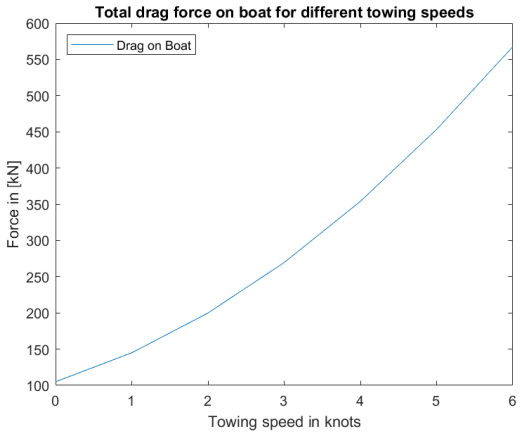

Figure 5.2: Total resistance on the tug for H_s=6.1 [m]

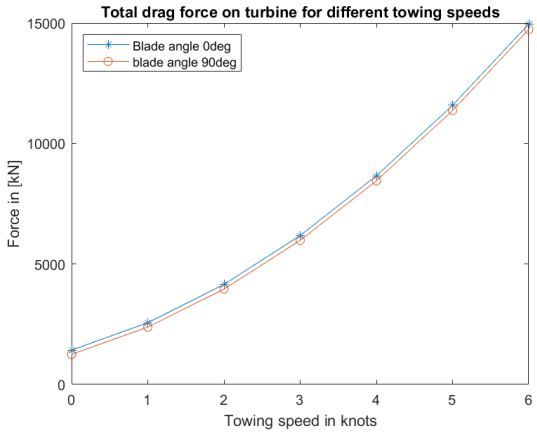

Figure 5.3: Total resistance on the Turbine for H_s=6.1 [m]

The individual weather components of the resistance on the FWT is seen in Figure 5.4. The underwater hull resistance due to current is shown as dominant. From Figure 5.5 which shows the components excluding the current, it can be seen that blade angle has a significant effect on blade resistance. The wave force is shown as constant as is should be, due to not taking into account the encounter frequency.

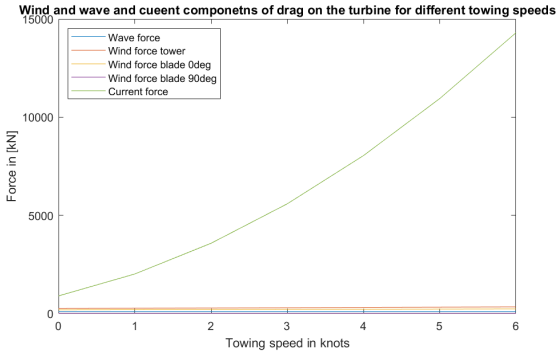

Figure 5.4: Components of the resistance on the turbine for H_s=6.1 [m]

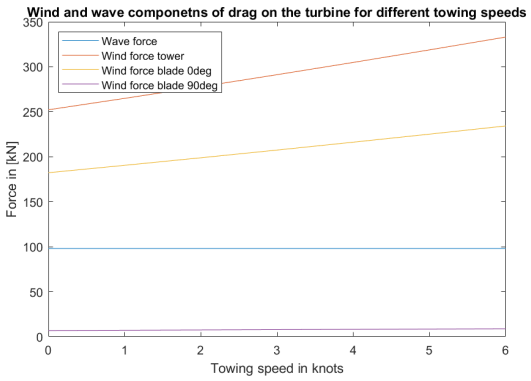

Figure 5.5: Wind and wave components of the resistance on the turbine for H_s=6.1 [m]

Figure 5.6 shows that the resistance due to current is less dominant on the tug then was seen for the FWT. The current is still clearly dominant for higher speed as expected, but is not dominant for low towing speeds.

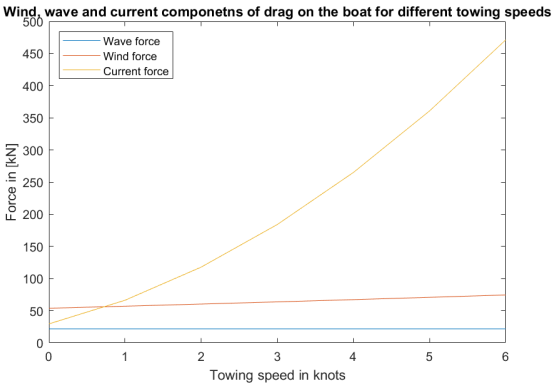

Figure 5.6: Components of the resistance on the tug for H_s=6.1 [m]

Table 5.2 shows a summery of the forces for a towing speed of 2 knots where the required propeller force was determined using the 90 degree blade angle due to the small reduction in drag.

Table 5.2: Forces acting on vessels for a towing speed of 2 knots and design weather conditioned

Force	[kN]
F_{rt}	199.8
F_{ro_0}	4149
$F_{ro_{90}}$	3958
F_P	4158

With a bollard pull of over 100 tonnes the MBL of the towline is given as

2 times the bollard pull from Table 3.1. Equation 3.11 then gives the minimum length requirement. The resulting towline and bollard pull requirements are shown in Table 5.3.

Table 5.3: Towline and bollard pull requirements for a towing speed of 2 knots in design weather condition

Parameter	Value	Unit
BP	424	[Tonnes]
$L_{towline_{min}}$	900	[m]
MBL	8316	[kN]
$d_{towline}$	100	[mm]
$\overline{T}$	3958	[kN]

Mild weather condition

The mild weather condition is quite similar to the design weather condition due to the dominance of the current forces which are the same. But due to the reduction in the other forces the current has become even more dominant. This is especially noticeable with regards to the forces acting on the tug for low towing speeds as shown in **??**. The reduction in wind speed has also reduced the effect of the blade angle.

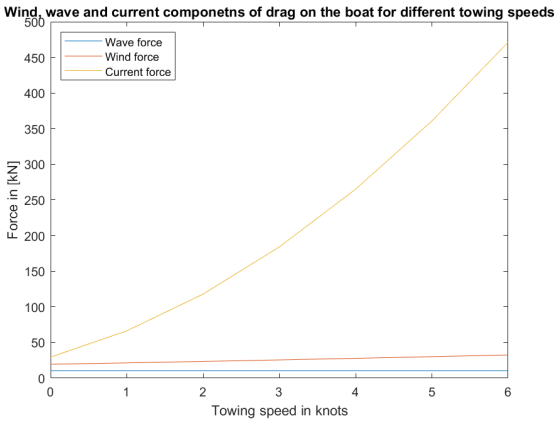

Figure 5.7: Components of the drift force on the boat for H_s=31 [m]

The resulting forces are fairly similar as for the design weather condition as shown in Table 5.4. The towing line parameters will be determined from the design weather condition but the required bollard pull and mean towing line tension for the mild weather condition is shown in Table 5.5

Table 5.4: Forces acting on vessels at a towing speed of 2 knots for the mild weather state

Force	[kN]
F_{rt}	151.6
F_{ro_0}	3727
$F_{ro_{90}}$	3799
F_P	3878.6

Table 5.5: Estimated mean towline and required bollard pull required at a towing speed of 2 knots for the mild weather condition.

Parameter	Value	Unit
BP	395	[Tonnes]
$\overline{T}$	3727	[kN]

5.2 Frequency response model MATLAB

The second model is used to estimate the maximum tension in the towing line. In order to do this the model uses the towline data and towing speed found using the first model. The maximum dynamic tension is estimated using the method outlined in subsection 3.6.1 and the maximum tension is found as shown in Equation 3.63. Matlab is used to perform the analysis

This model builds on the static model by including the linear wave forces on the tug. as mentioned in chapter 5 one of the three models also takes into account a linearized version of the drag on the towing line. This is done using the linearization shown in subsection 3.6.1. The analysis was performed using Matlab.

The towline was modelled using a weight in water of 0.87 times the weight in air for steel wire rope based on recommendations found in the SIMO user manual. [22]. The elastic modulus of steel wire rope and corresponding drag coefficient was chosen based on recommendations in DNV-OS-E301, [23]. The nominal cross section was determined from the provided hardware catalogue. The towline length was chosen as two times the minimum length. The resulting line data is shown in Table 5.6.

The required computation time for the fifth model turned out to be quite significant due to this a simulation time of 3 hours was used instead of the planed operation length of 65 hours or the 97.5 hours including a contingency factor of 1.5. 3 hours is the duration of a sea state and was therefore selected. in order to provide a foundation better for comparison 3 hours was used for all models. For the time domain models 20 seeds was used in order to generate the Gumbel distribution.

Table 5.6: Towline data used in model 2.

Parameter	Value	Unit
$\overline{T}$ design weather	3958	[kN]
$\overline{T}$ mild weather	3727	[kN]
w_{air}	48.2	[kg/m]
w	383	[N/m]
$d_{towline}$	100	[mm]
$A_{towline}$	$5740 \cdot 10^{-6}$	$[m^2]$
E	$7 \cdot 10^{10}$	$[N/m^2]$
$C_{d_{line}}$	1.6	[]
$L_{towline}$	1800	[m]

5.2.1 Results and discussion

The approach angel for the towing line ϕ was found using Equation 3.34 as 0.0043 rad. Figure 5.8 shows the resulting RAO for the along line motion relative to wave height. As expected for such a small angel the RAO is quite similar to the surge motion RAO. This means that the heave and pitch motions of the vessel will have a very small effect on the motion along the towline.

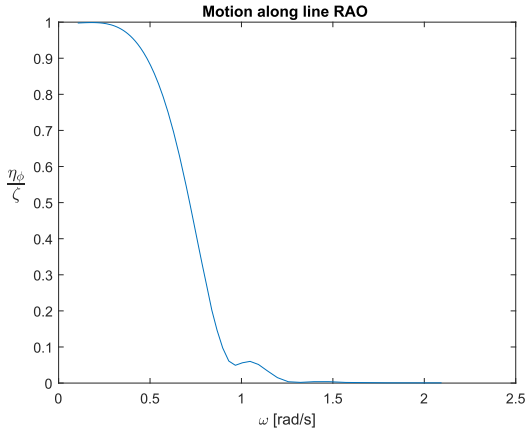

Figure 5.8: Motion along line RAO

Figure 5.15 and 5.16 show the resulting motion spectrum for the motion along the line found using Equation 3.59. This shows a significant difference in the expected motions of the tug for the different weather conditions. This is expected due to the much larger sea state. Due to this model only taking into account dynamic motion due to wave the change in wind velocity is not effecting the results. The change in wind has a small effect on the mean towline tension from model 1 but that was quite small.

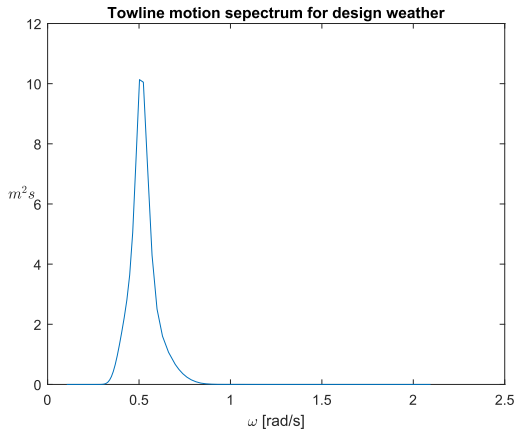

Figure 5.9: Spectre for line motion in design weather

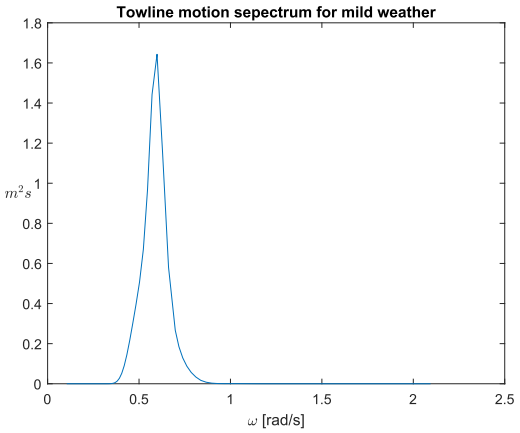

Figure 5.10: Spectre for line motion in mild weather

The elastic towline stiffness is not effected by the weather condition due to maintaining the same towing line, but there is a small difference in geometric stiffness resulting in a small variation in total stiffness. The towline stiffness including drag changes significantly more for the weather states as shown in Figure 5.11 and 5.12. For the mild weather the stiffness lower as expected due to there being less movement on the tug and as such less damping. The drag stiffness is between the total and elastic stiffness which is expected. Further more the elastic stiffness is the larges and thus conservative also as expected.

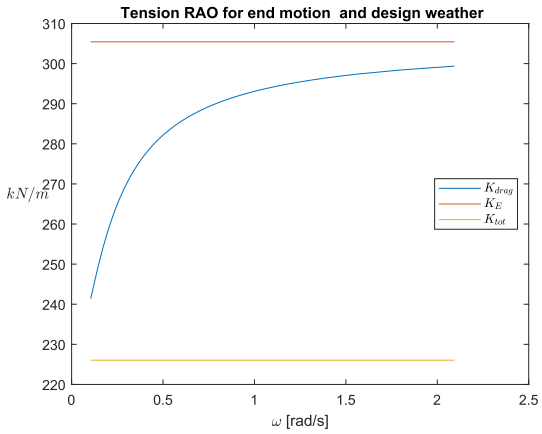

Figure 5.11: Tension in line due to line motion RAO for design weather

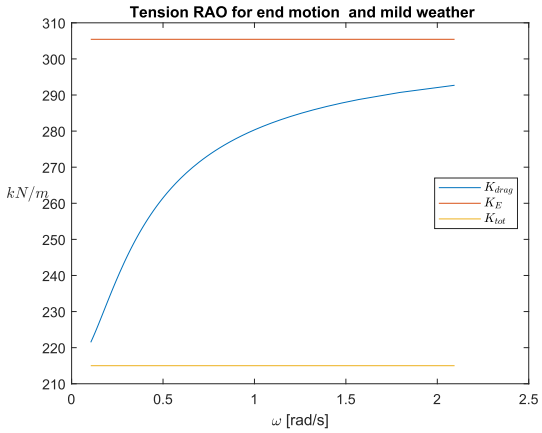

Figure 5.12: Tension in line RAO due to line motion for mild weather

Figure 5.13 and 5.14 shows the same trends with regards to the different stiffness models and weather conditions, as tension due to wave motion RAO. But here we see the models converge due to the value for the motion RAO going towards zero for high frequencies. The peaks are all located quite close to the peak of the motion spectra.

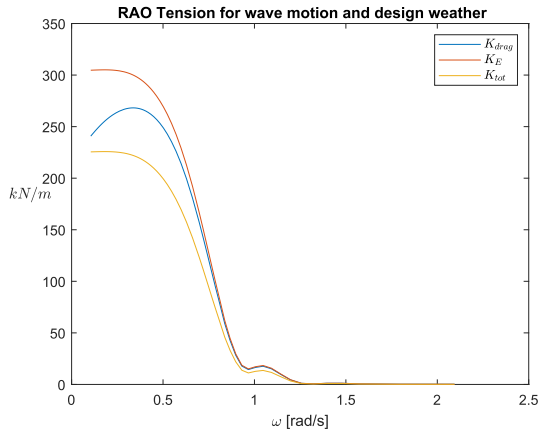

Figure 5.13: Tension in line due to wave motion RAO for design weather

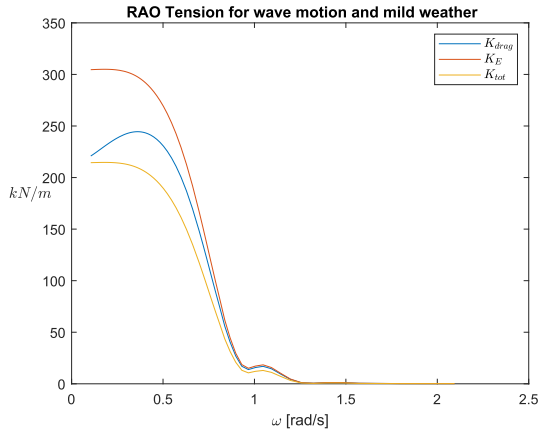

Figure 5.14: Tension in line due to wave motion RAO for mild weather

Figure 5.15 and 5.16 shows the resulting tension spectres showing the expected trends with regards to both the line stiffness model and the weather condion. Table 5.7 and 5.8 shows the standard deviation for the spectra and corresponding MPM tension. The standard deviation is shown as significantly larger for the design weather condition as expected, due to the corresponding motion spectrum having a significantly more energy but a similar distribution. The resulting tensions show that the drag has significant effect on the dynamic tension for both the design and mild weather conditions. Mean towline tension is clearly significantly larger for all cases, ensuring that the line won't go slack. The MPM total tension maxes out at 63.56% of the MBL for the design weather and 51.48% for the mild weather. For the drag model the percentages are slightly lover 62.38% and 50.63% respectively. Both cases for the design weather condition gives a significant safety margin, this is good as the MPM is not a conservative estimate for a given condition.

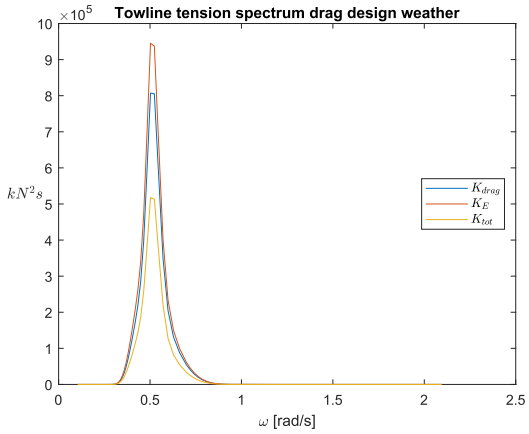

Figure 5.15: Spectrum for line tension in design weather

Table 5.7: Spectra parameters for design weather

Towline model	$\sigma_{tension}$ [kN]	$T_{D_{MPM}}$ [kN]	$T_{tot_{MPM}}$ [kN]	% of MBL
K_E	354	1328	5286	63.56
K_{tot}	262	983	4941	59.42
K_D	328	1230	5188	62.38

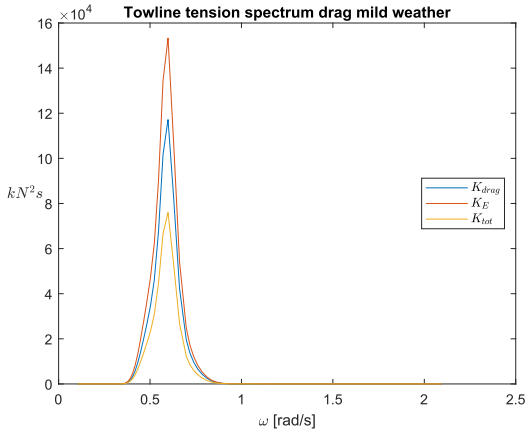

Figure 5.16: Spectrum for line tension in mild weather

Table 5.8: Spectra parameters for mild weather

Towline model	$\sigma_{tension}$ [kN]	$T_{D_{MPM}}$ [kN]	$T_{tot_{MPM}}$ [kN]	% of MBL
K_E	1.46	554	4281	51.48
K_{tot}	1.03	390	4117	49.51
K_D	1.27	483	4210	50.63

5.3 Time Domain analysis

The wave responses was assumed Rayleigh distributed. When determining the resulting Gumbel distribution 20 wave seeds was used. The length of the time domain analysis was set to 3 hours as this is the length of a sea state. Originally the planed operation time was intended to be used but doe to the computation time required for the coupled SIMO/RIflex analysis it was reduced to 3 hours.

5.3.1 Separated analysis models SIMO

The third and fourth model uses SIMO to perform time domain analysis using separation of motion on the tug. This is done in order to determine the dynamic response of the tug and the resulting tension in the towing line. SIMA is used to sett up and run the SIMO analysis. The models are sett up as a mass representing the tug connected to a fixed point representing the FWT. A catenary line is used to connect them representing the towing line. The forces acting on the FWT is taken in to account through the bollard pull found in the first model. this is done by setting the bollard pull as a specified force on the tug. The model uses the same towing line parameters as the second model. In order to ensure continues head weather the tug is lock in sway, roll and yaw.

The modelling of the catenary line is what separates the models the third model uses the shooting method, while the fourth uses the shooting method including simplified line dynamics. The shooting method is a two dimensional method. The line is assumed to remain in a vertical plane containing both end points. The pure quasistatic model of the third model the effects of transverse drag forces on the line are neglected. The total line tension and the angle of the upper end are determined by the locations of the end points relative to each other. A two dimensional line characteristics table is calculated. The simplified line dynamics model is based on four important assumptions, [24].

1. Only the tangential component of the top end motion is assumed to have any effect on the dynamic tension
2. The shape of the dynamic motion due to a tangential excitation is assumed to be equal to the change in static line geometry.
3. Mass forces on the line are neglected.
4. The elastic elongation of the line is determined quasistatically.

5.3.2 Total motion SIMO/RIFLEX

The fifth model uses a coupled SIMO/RIFLEX analysis to determine the dynamic response of the tug and the resulting tension in the towing line. This is a total motion time analysis in the time domain. The model is setup the same way as the third and fourth models except that the line is modelled using FEA in RIFEX instead of a catenary line. The line is modelled using the same towing line parameters as the second model. Due to this the coupled SIMA/RIFLEX model is presumed to be the

most accurate model. SIMA is used to set up and run the coupled SIMO/RIFLEX analysis. The FEA analysis was performed for 200 elements resulting in a element length of 9 meters.

5.3.3 Results and discussion

Static results

Table 5.9 shows the resulting mean static forces on the tug for both the separated motion and the total motion models. The static solver in SIMO gives the same results for both towline models therefore they are given together. These results match very well with the results from the first model. This verifies the first models analysis of the mean forces on the tug. The analysis on the forces acting on the FWT is not evaluated by any of the time domain analysis. The difference in the static towline tension is due to the solver not finding a perfect equilibrium. The negative values is due to the forces acting in negative surge direction in order to compensate for the specified bollard pull.

Table 5.9: Static forces from SIMA

Static forces on tug	Wave drift	Wind	Current	Total	Towline
Design weather SIMO	-21.66	-60.15	-117.8	-199.61	-3956
Design weather SIMO/RIFLEX	-21.66	-60.15	-117.8	-199.61	-3980
Mild weather	-10.46	-23.24	-117.8	-151.5	-3724
Mild weather SIMO/RIFLEX	-10.46	-23.24	-117.8	-151.5	-3760

Dynamic results

The following results are all from the same wind and wave seed. Only one seed is presented, due to the results all following the same patterns regardless of seeds.

Figure 5.17 shows the surge motion for the different models around the motion peak for design weather condition. The separated analysis models match quite well with only small differences. The coupled total motion analysis on the other hand gives slightly lower motion amplitude but has the same general shape. The fast Fourier transforms of the motions shown a reduction in energy at large periods for both the simplified dynamic model and the coupled model as shown in Figure 5.18. This could be due to the low frequency damping due to relative wind and current velocities as outlined in 3.65 and Equation 3.66. The FFT shows that the coupled analysis reduces the energy at large periods slightly more than the simplified model does. But this difference is smaller than the difference between the simplified and shooting models, and is therefor not believed to be the sole cause of the smaller surge motions for the coupled model. The coupled model takes into account the effect of mass and drag forces from the towing line on the tug motions unlike the other models. This might be contributing to the difference in motion.

Figure 5.17: Time realisation of surge motion for design weather

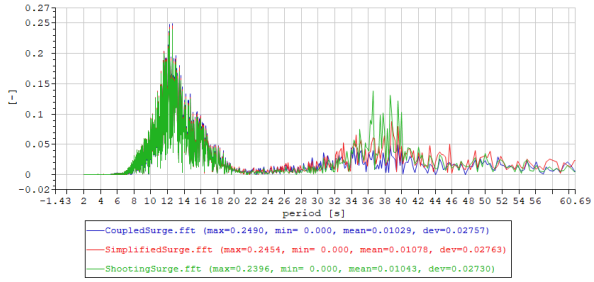

Figure 5.18: Fast Fourier transform of time realisation of surge motion for design weather

Figure 5.19 and 5.20 shows the heave and pitch motion of the tug for the different models. The difference in motion is negligible. Due to this the differences in the FFTs for the different models are also negligible. Therefore heave and pitch motion FFTs are shown for the shooting method only in Figure 5.21. Which shows that the heave and pitch has no energy at the larger periods. The heave and pitch motion does not result in as large motions in the towing line as the surge motion does. Therefor the lack of significant difference in motion for the coupled model could be caused by the reduction in both high frequency forces and line motions.

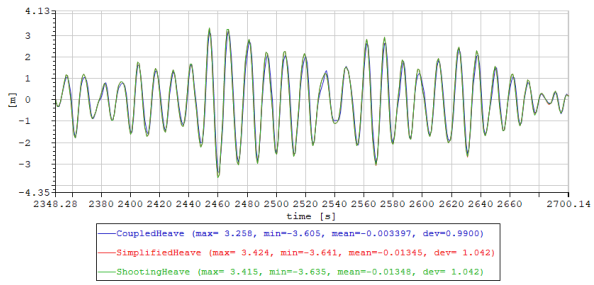

Figure 5.19: Time realisation of heave motion for design weather

Figure 5.20: Time realisation of pitch motion for design weather.

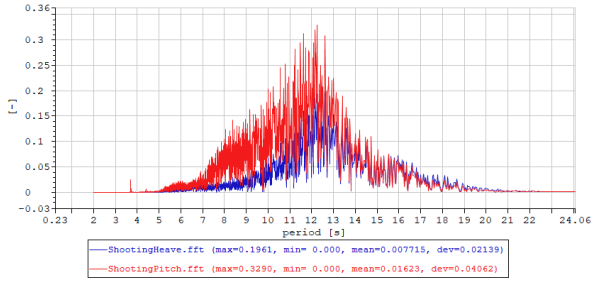

Figure 5.21: Fast Fourier transform of time realisation of heave and pitch motion for design weather from shooting method

The mild weather motion responses of the tug follow the same trends as the design weather responses, but with smaller amplitudes. The main difference is that difference in surge motion between the coupled model and the others, have become slightly more significant as shown in Figure 5.22.

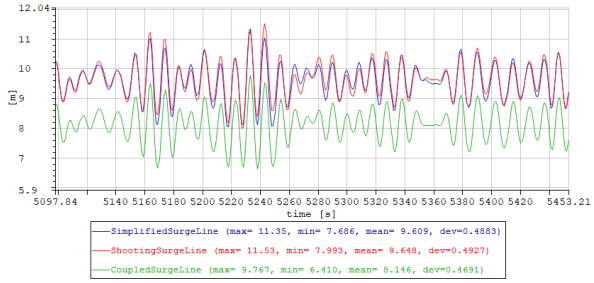

Figure 5.22: Time realisation of heave motion for mild weather

Figure 5.23 shows the heave motion of the towline node closest to the tug for the shooting method. This is obviously incorrect the motion seems to move between a upper and lower boundary with no time spent in between. The difference between the upper and lower bound is also much smaller than would be expected based on the heave motion. The reduction in heave motion could be caused by the pitch motion. But that would still not explain the sudden jumps

from either the upper or lower bound to the other. Figure 5.24 shows the visualisation of the tug and line motions. The line is shown with a bend, which is should definitely not have. In order to ensure the pitch motion is not causing the problem the analysis was performed with the towline attached at the COG. This resulted in the same irregularities therefor there must be another cause. The problem was also found for the simplified dynamics method. After a discussions with my supervisor it is believed that the cause of this is the pregenerated tables used in both methods to determine the towline tension. The tables are generally 2-dimensional on the form Tension vs x position for given values of z. For quasi-static methods it is common not to change the vertical position, z resulting in a correlation between tension and the x position. This results in the towline motion not taking into account the heave motion of the vessel and only being dependent on the surge motion. The frequency response method showed that the tug heave and pitch motion had a very limited effect on the motion along the towline, and as such the towline tension. Figure 5.25 shows the surge motion of the node and it looks as expected compered to the corresponding surge motion of the tug.

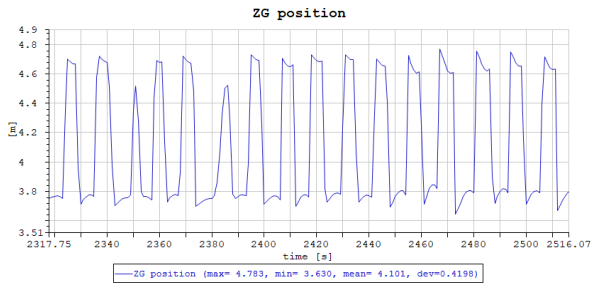

Figure 5.23: Time realisation of heave motion at towline end near tug for SIMO shooting model at design weather condition

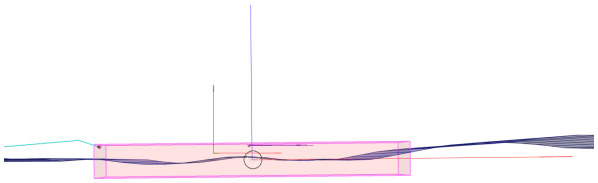

Figure 5.24: Visualisation of the tug and line motion for SIMO shooting model at design weather condition

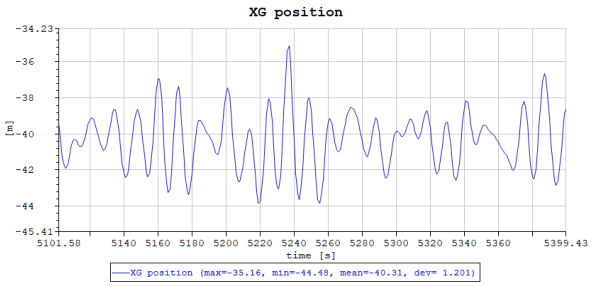

Figure 5.25: Time realisation of surge motion at towline end near tug for SIMO shooting model at design weather condition

Figure 5.26 and 5.27 shows the fast Fourier transforms of the motion at the centre of the line. As for the vessel motion the high period energy is damped for the coupled and simplified model compered to the shooting model. For the heave motion the coupled model is damped for the wave period energy as well. While for the surge motion the energy is slightly higher for the coupled model at the wave periods. The mild weather results mirror this but with slightly less damping of the high periods for the coupled and simplified models. Figure 5.28 shows the FFT of the line tension, It is observed that this follows the same trends as the FFT of the surge motion. Which is consistent with the frequency domain model in that the line tension is mostly dependent on surge motion.

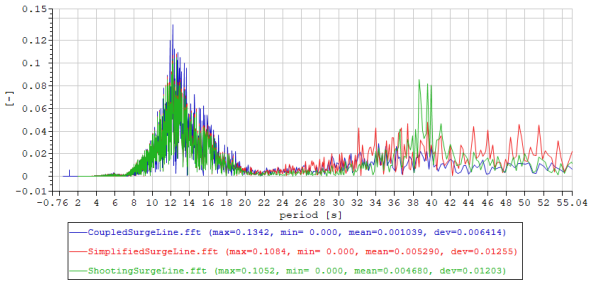

Figure 5.26: Fast Fourier transform of surge motion at centre of line for design weather

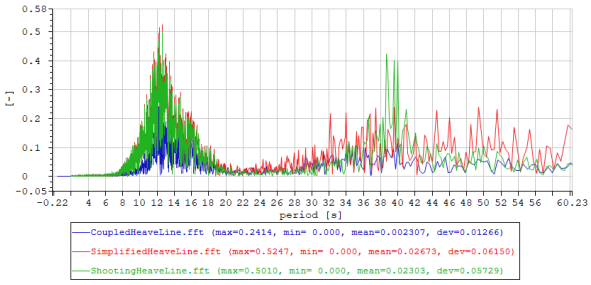

Figure 5.27: Fast Fourier transform of heave motion at centre of line for design weather

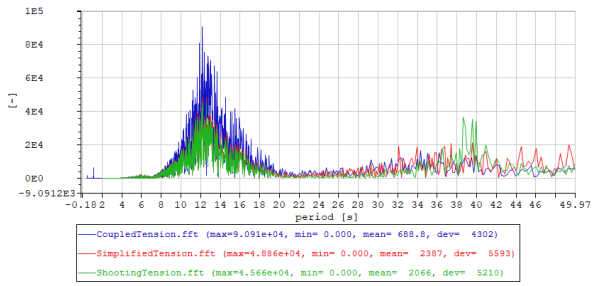

Figure 5.28: Fast Fourier transform of tension in line for design weather

Figure 5.29 and 5.30 shows the time realisation of the line tension for the design and mild weather conditions respectively. Both show a similar shape with regards to periods and variation. But while the design weather condion results in a higher tension for the coupled model the mild weather gives the highest tension for the simplified model. This difference is probably due to the inaccuracies in the simplified model with regards to towline drag has a larger relative effect for calmer weather.

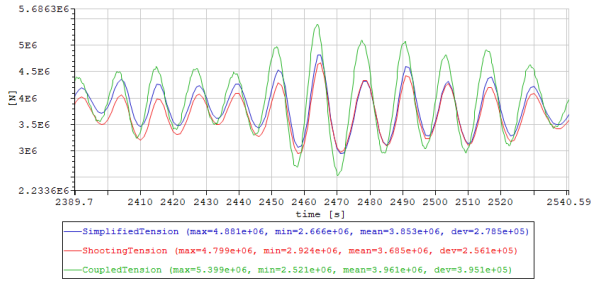

Figure 5.29: Time realisation of the tension in the line for the design weather

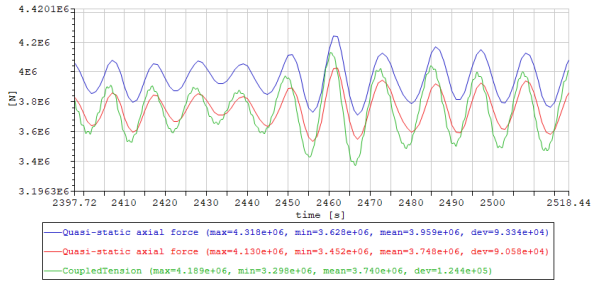

Figure 5.30: Time realisation of the tension in the line for the mild weather

Figure 5.31 shows the resulting Gumbel distribution for the extreme towline tensions. For the design weather condition the coupled analysis is shown giving the largest tension and with the least variation. But for the mild weather condition it is shown as having the most variation and only the second largest tension. The Simplified dynamics model on the other hand is the other way around, with the

second largest tension and the least variation for the design weather. While having the largest tension and least variation for the mild weather condition. The shooting model is shown as consistently giving the least tension and a middle variation for both conditions. The simplified drag model is supposed to be conservative which consists with the result for the mild weather. While for the design weather the simplified model does not provide a conservative estimate. This indicates that other dynamic effects than drag have a significant effect. Such as the towline mass forces. Table 5.10 shows some of the main characteristics of the distributions.

For both weather conditions the frequency response model is closer to the coupled model than the simplified model. This is unexpected a the simplified line dynamics is expected to be more precise model of the drag on the towline. While the simplified model requires much less computation time then the coupled model it still requires much more than the frequency response model and is expected to be more precise. The shooting model gives fairly similar results as the combined elastic and geometric stiffness model using frequency response as expected.

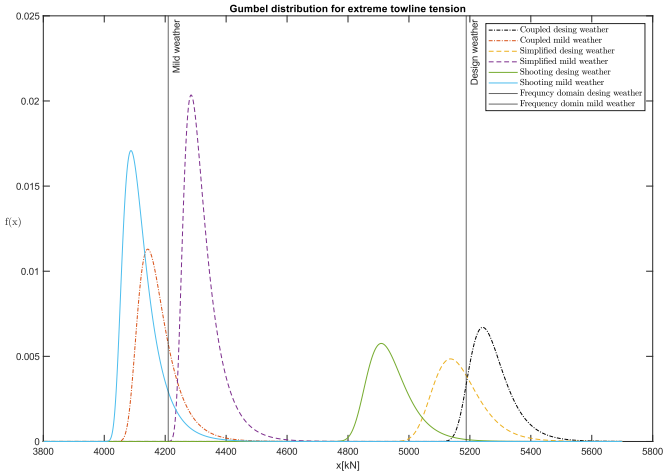

Figure 5.31: Gumbel distribution of the extreme tension in the towing line

Table 5.10: Statistical properties of the extreme tension Gumbel distribution

Analysis model	$\sigma_{max_{tension}}[kN]$	$T_{tot_{MPM}}$ [kN]	% of MBL	90% fractile
Shooting design	68,98	4909	59.03	5022
Simplified design	95.70	5145	61.87	5251
Coupled design	58.35	5242	63.04	5362
Shooting mild	27.31	4088	49.16	4232
Simplified mild	24.01	4285	51.53	4436
Coupled mild	37.30	4143	49.82	4273

Chapter 6

Conclusions and Recommendations

A literature review of state-of-art concepts for offshore towing have been performed in combination with a review of selected towing accidents. The information gathered has then been used to perform an analysis, on the towing of the Hywind Tampen FWT from Gulen to the Tampen field. For this analysis several models with varying complexities has been created. The models span from a simple static model to a coupled SIMA/RIFLEX time domain model.

Harsh weather was a common factor for the high consequence accidents. This illustrates the importance of understand the weather in the area and the dynamic responses of the system connected with it.

The static model showed that the mean towline force was dominated by the drag current on the FWT. And that the effect of the pitch angle of the blades is quite small.

The frequency response model gives relatively accurate results while requiring very little calculation time. This makes it well suited for an early design phase. Its low calculation time combine with the simplicity of the model makes it well suited for the changes that happen during an early design phase. Due to this the frequency response model is recommended for early phase estimates. But for later stages of the planing when the accuracy of the model becomes critical and less changes are expected the coupled SIMA/RIFLEX is recommended.

While the frequency response model gave quite good results in this analysis it must be considered that it does not take into account high frequency dynamic loads from wind or wave drift. This can for certain sea states cause the quality of the model to decrease. Emphasising the need to understand the weather in which the operation is planed.

The coupled SIMA/RIFLEX model gives a maximum tension of 5242 kN which is 63.04% of the MBL of the towing line, which corresponds to a safety factor of approximately 1.59. This shows that the combination of a very simple model and rules and regulation gives a respectable safety factor for sizing of the towline.

6.1 Recommended further work

In order to test the assumption that the motions of the FWT can be neglected further research into the effect of those motion on the towline tension is recommended. A two body coupled SIMO/RIFLEX analysis would give interesting insight on the subject. The effect of neglecting the encounter frequency would also be an interesting proposition for future research.

Research into the probability of towline failure for a towline design using the current rules and regulations is recommended.

Bibliography

[1] DNV, 'Dnv-os-h101 marine operations, general,' 2011.

[2] DNV, 'Dnv-os-h202 sea transport operations (vmo standard - part 2-2),' 2015.

[3] I. J. Fylling, 'Analysis of towline forces in ocean towing systems,' 1979.

[4] F. G. Nielsen, *Lecture Notes in Marine Operations*. 2007.

[5] DNV, 'Dnv-rp-h103 modelling and analysis of marine operations),' 2014.

[6] T. H. Risoey, H. Mork, H. Johnsgard and J. Gramnaes, 'The pencil buoy method-a subsurface transportation and installation method,' Offshore Technology Conference, 2007. DOI: 10.4043/19040-MS.

[7] M. L. Fernàndez, 'Tow techniques for marine pipeline installation,' 1981.

[8] K. Larsen, *Tmr4225 marine operations, lecture notes #3 – towing operations*, 2020.

[9] E. Skaug, 'Sleping av rigger. tekna seminar posisjonering av plattformer og skip,' 1993.

[10] UK Government, *Marine accident investigation branch reports*. [Online]. Available: https://www.gov.uk/maib-reports?keywords=tow.

[11] T. E. Berg and Ø. Selvik, 'Emergency towing operation in arctic waters,' 2015.

[12] US Coast Guard, 'Report on investigation into the circumstances suttounding the multiple related marine casualties and grounding of the modu kulluk on december 31, 2012,' 2014.

[13] K. Larsen, *Tmr4225 marine operations lecture notes #7a – operability and weather windows*, 2020.

[14] O. M. Faltinsen, *Sea loads on ships and offshore structures*. Cambridge University Press, 1990.

[15] S. Steen, *Lecture Notes in Experimental Methods in Marine Hydrodynamics*. 2014.

[16] K. Larsen, *Time domain analysis overview*.

[17] Equinor, *Hywind tampen facts*. [Online]. Available: https://www.equinor.com/en/what-we-do/hywind-tampen.html.

[18] Skipsrevyen.no, *Skipsrevyen data for m/s normand ferking*, 2021. [Online]. Available: `https://www.skipsrevyen.no/batomtaler/m-s-normand-ferking/`.

[19] P. H. Bastiaanssen, *Modelling the dynamic behaviour of a rotor nacelle assembly during installation using a floating vessel*, 2020.

[20] Equinor, 'Snorre field metocean design basis,' 2016.

[21] DNV, 'Dnv-rp-c205 environmental conditions and environmental loads,' 2014.

[22] SINTEF Ocean, 'Simo 4.18.1 user guide,' 2020.

[23] DNV, 'Dnv-os-e301 position mooring,' 2018.

[24] SINTEF Ocean, 'Simo 4.18.1 theory manual,' 2020.

Appendix A

Abbreviations

DNV Det Norske Veritas
JONSWAP Joint North Sea Wave Project
SIMA Simulation Workbench for Marine Appications
SIMO Simulation of Marine Operations
CDT Controlled Depth Tow
WoW Waiting on Weather
FWT Floating Wind Turbine
RAO Response Amplitude Operator
MBL Minimum Braking Load
NTNU Norwegian University of Science and Technology
COG Centre of gravity
MPM Most probable maximum

Appendix B

MATLAB codes

B.1 Static force

```
% --------------------------------------------------------------------------
%                       MAIN FILE - Static force
% --------------------------------------------------------------------------
%
% Calculate the static force acting on the towing line
%
%
%
%   Name                Description
% --------------------------------------------------------------------------
%
% --------------------------------------------------------------------------
%   catman_read_dt.m    Function to open binary files.
%
% Programmed:           Martin Mongstad Hope  (November 2020)
% --------------------------------------------------------------------------
clc
clear all
close all

T=[12.2];% wave peak periods orginal 12.2 10
H=[6.1]; %wave hight orginal 6.1  3

rho_air=1.27;  %kg/m^3 Faltinsen page 175
rho_water=1025; %kg/m^3
Cd_air_turbine=1;
Cd_water_turbine=1;
Cm_water_turbine=1;
% C_D_tug=-0.00153308351400000;
C_M_tug=1;
% Towing_speed_in_knots=0; % knots
Wind_speed_at_10m=17.5; % m/s orginal 17.5   10.5
z_0=0.01;      %  DNV-RP-C205 Terrain roughness parameter table 2-1...
%  worst case open sea with waves
wave_period=12.2; %s
wave_hight=6.1; %m
current_speed=2; %knots tampen= 2
X=[0:1:6];
t=1;
```

```
for i=0:6
    Towing_speed_in_knots=i; % knots
Fd_turbine_wind(t) = Force_on_the_turbine(Towing_speed_in_knots,...
    Wind_speed_at_10m,z_0,rho_air,Cd_air_turbine)*10^(-3);

Fd_turbine_drag(t)= Current_drag_on_turbine(Towing_speed_in_knots,...
    current_speed,rho_water,Cd_water_turbine)*10^(-3);

[Force_D_0(t),Force_D_90(t),Force_L_0(t),Force_L_90(t)] = ...
    (Force_on_the_blades(Towing_speed_in_knots,Wind_speed_at_10m,z_0));

Fd_turbine_wave(t) = Drift_on_the_turbine(Towing_speed_in_knots,T,H,...
    rho_water)*10^(-3);



Fd_turbine_total_0deg(t)=Fd_turbine_wave(t)+Force_D_0(t)+...
    Fd_turbine_drag(t)+Fd_turbine_wind(t);

Fd_turbine_total_90deg(t)=Fd_turbine_wave(t)+Force_D_90(t)+...
    Fd_turbine_drag(t)+Fd_turbine_wind(t);


Fd_boat_drag(t)=abs(Dragcoeficient_boat(Towing_speed_in_knots,...
    current_speed));

Fd_boat_wind(t) = abs(Force_on_the_boat(Towing_speed_in_knots,...
    Wind_speed_at_10m));

Fd_boat_drift(t) =abs( Drift_on_the_boat(T,H));



Fd_boat_total(t)=abs(Fd_boat_wind(t) +Fd_boat_drag(t)+...
    Fd_boat_drift(t));







Fd_total_0deg(t)=Fd_turbine_total_0deg(t)+Fd_boat_total(t);

Fd_total_90deg(t)=Fd_turbine_total_90deg(t)+...
    Fd_boat_total(t);
t=t+1;

end
figure
plot(X,Fd_total_0deg,'-*',X,Fd_total_90deg,'-o')
title('Total drag force on system for different towing speeds')
xlabel('Towing speed in knots')
ylabel('Force in [kN]')
legend('Blade angle 0deg','blade angle 90deg','Location','northwest')

figure
plot(X,Fd_boat_total)
title('Total drag force on boat for different towing speeds')
xlabel('Towing speed in knots')
ylabel('Force in [kN]')
```

```
legend('Drag on Boat','Location','northwest')

figure
plot(X,Fd_turbine_total_0deg,'-*',X,Fd_turbine_total_90deg,'-o')
title('Total drag force on turbine for different towing speeds')
xlabel('Towing speed in knots')
ylabel('Force in [kN]')
legend('Blade angle 0deg','blade angle 90deg','Location','northwest')
%
figure
plot(X,Fd_turbine_wave,X,Fd_turbine_wind,X,Force_D_0,...
    X,Force_D_90,X,Fd_turbine_drag)
title('Wind and wave and cueent componetns of drag on the turbine for'...
    'different towing speeds')%
xlabel('Towing speed in knots')
ylabel('Force in [kN]')
legend('Wave force','Wind force tower','Wind force blade 0deg',...
    'Wind force blade 90deg','Current force','Location','northwest')

figure
plot(X,Fd_turbine_wave,X,Fd_turbine_wind,X,Force_D_0,...
    X,Force_D_90)
title('Wind and wave componetns of drag on the turbine for different'...
    'towing speeds')%
xlabel('Towing speed in knots')
ylabel('Force in [kN]')
legend('Wave force','Wind force tower','Wind force blade 0deg',...
    'Wind force blade 90deg','Location','northwest')

%
figure
plot(X,Fd_boat_drift,X,Fd_boat_wind,X,Fd_boat_drag)
title('Wind, wave and current componetns of drag on the boat for'...
'different towing speeds')
xlabel('Towing speed in knots')
ylabel('Force in [kN]')
legend('Wave force','Wind force','Current force','Location','northwest')
```

B.2 Wind speed

```
% ------------------------------------------------------------------------
%             MAIN FILE - Calculating the force on the Blades
% ------------------------------------------------------------------------
%
%    Calculate the wind speed for difrent hights
%
%
%
%   Name                Description
% ------------------------------------------------------------------------
%
% ------------------------------------------------------------------------
%
% Programmed:           Martin Mongstad Hope  (November 2020)
% ------------------------------------------------------------------------
```

```
function [wind_speed] = Wind_speed(Wind_speed_at_10m,z,z_0)
a=0.12;
%UNTITLED3 Summary of this function goes here
%   Detailed explanation goes here
% wind_speed = Wind_speed_at_10m*(1+(log(z/10)/log(10/z_0))); %
  wind_speed = Wind_speed_at_10m*(z/10)^(a) ;% alternativ formel a=0.12 dnv
%  1/7 fra kjell
end
```

B.3 Current drag on turbine

```
% -------------------------------------------------------------------------
%             MAIN FILE - Calculating the force on the turbine
% -------------------------------------------------------------------------
%
%    Calculate the drag and lift forces acting on the turbine exskluing
%    the blades
%
%
%   Name                Description
% -------------------------------------------------------------------------
%
% -------------------------------------------------------------------------
%
% Programmed:           Martin Mongstad Hope  (November 2020)
% -------------------------------------------------------------------------
function [Fd] = Current_drag_on_turbine(Towing_speed_in_knots,...
    current_speed,rho_water,Cd_water)
%UNTITLED5 Summary of this function goes here
%   Detailed explanation goes here

Towing_speed_in_ms=Towing_speed_in_knots*0.514444;%the towing speed in m/s
Current_speed_in_ms=current_speed*0.514444;
Current_speed_tot=Towing_speed_in_ms+Current_speed_in_ms;
depth=90;% draught in meters
D=18.3; % substructure diameter m
    c_cur=0.5*Cd_water*rho_water*D*depth;
    Fd=0.5*Cd_water*rho_water*D*depth*Current_speed_tot^2;
end
```

B.4 Force on the turbine

```
function [Fd] = Drift_on_the_turbine(Towing_speed_in_knots,...
    T_0_turbine,H_S,rho_water)
%UNTITLED5 Summary of this function goes here
%   Detailed explanation goes here
g=9.81;
depth=18.3;
D=18.3;
R=D/2;

zeta_a=1;  % enhets bølge (Kjell)
Towing_speed_in_ms=Towing_speed_in_knots*0.514444;%the towing speed in m/s
```

```
omega_0=2*pi/T_0_turbine;
omega_e=omega_0+(omega_0^2)*Towing_speed_in_ms/g;
T_1=2*pi/omega_e;
T_1=0.834*T_0_turbine;

F1_del=[0 0 0.014 0.0285 0.043 0.07     0.129 0.18 0.243 0.3 0.357...
    0.414 0.471];
F1=F1_del.*(0.5*rho_water*g*(zeta_a^2)*D);%
omega_graf=[0.001 0.1 0.2 0.3 0.4 0.5 0.6 0.7 0.8 0.9 1 1.1     1.2];
delta_omega=sqrt(0.1*g/R);

omega_graf.*g./R;

    tel=1;
    for i=omega_graf
        omega=sqrt(omega_graf(tel)*g/R);




    if omega <= 5.24/T_1
        sigma=0.07;
    else
        sigma=0.09;
    end
    Y=exp(-(((0.191*omega*T_1)-1)/(sqrt(2)*sigma))^2);

    S(tel)=155*((H_S^2)/((T_1^4)*(omega^5)))*exp(-944/((T_1^4)*...
        (omega^4)))*((3.3)^(Y));
    tel=tel+1;
    end

    gggg=sum(S);

    Fd=2*sum(delta_omega.*F1.*S);
end
```

B.5 Force on the blades

```
% -------------------------------------------------------------------------
%             MAIN FILE - Calculating the force on the Blades
% -------------------------------------------------------------------------
%
%    Calculate the drag and lift forces acting on the Blades
%
%
%
%   Name                Description
% -------------------------------------------------------------------------
%   Z_0  DNV-RP-C205 Terrain roughness parameter table 2-1...
               %  worst case open sea with waves
% -------------------------------------------------------------------------
%
% Programmed:           Martin Mongstad Hope  (November 2020)
% -------------------------------------------------------------------------
function [Force_D_0_tot,Force_D_90_tot,Force_L_0_tot,Force_L_90_tot] = ...
```

```
    Force_on_the_blades(Towing_speed_in_knots,Wind_speed_at_10m,z_0)
%UNTITLED5 Summary of this function goes here
%   Detailed explanation goes here

Towing_speed_in_ms=Towing_speed_in_knots*0.514444;% the towing speed in m/s
Blade_angles=[(pi)/3 pi 5*pi/3]; % anges of the blades...
% relative to the z_axsis
Hub_high=105;% hub hight from waterline in meters


%Hubradius=3.098;
%HubdragCoeficienttotal=0.085841;
datapoints_0deg_orgginal=[0 3.121495327 10.4375 20.875 31.3125 41.75...
    52.1875 62.625 73.0625 83.5 ; 0 0.093645 0.078037 0.039019 0.019509...
    0.007804 0 0 0 0; 0.085841 0.296542 0.327757 0.366776 0.31215...
    0.280935 0.265327 0.226308 0.171682 0.117056];


datapoints_0deg=datapoints_0deg_orgginal./(10^2); % radial length from
                                % seter of hub in row 1
                                % lift coeficient in row 2
                                % drag ceficient in row 3
                                % all data for 0 deg pitch angle
datapoints_90degorginal=[0 3.121495327 10.4375 20.875 31.3125 41.75 ...
    52.1875 62.625 73.0625 83.5; 0 -0.24972 -0.23411 -0.15607 -0.01562...
    0.023411 0.070234 0.078037 0.078037 0.039019; 0.085841 0.039019...
    0.039019 0.015607 0.007804 0.003902 0 0 0 0];%


datapoints_90deg=datapoints_90degorginal./(10^2);%
                        % radial length from seter of hub in row 1
                        % lift coeficient in row 2
                        % drag ceficient in row 3
                        % all data for 0 deg pitch angle
% figure
% plot(datapoints_90deg(1,:).*(10^2),datapoints_90deg(3,:),'-*', ...
% datapoints_0deg(1,:).*(10^2),datapoints_0deg(3,:),'-o')
% title('Drag Coeficient per length')
% xlabel('r [m]')
% ylabel('Drag Coeficient [Tonne/m^2]')
% legend('Blade angle 0deg','Blade angle 90deg','Location','northeast')
%
%
Steppsize=(25/2)*0.535*0.780374;

Force_D_0=zeros(1,9);
Force_L_0=zeros(1,9);
Force_D_90=zeros(1,9);
Force_L_90=zeros(1,9);


for j = 1:3
for i = 1:9
    if i==1
        z=Hub_high+cos(Blade_angles(j))*((datapoints_0deg(1,i+1).*(10^2)...
            +(datapoints_0deg(1,i+1).*(10^2)-Steppsize/2))/2);
    else
        z=Hub_high+cos(Blade_angles(j))*(datapoints_0deg(1,i+1).*(10^2));
    end
    wind_speed_z=Wind_speed(Wind_speed_at_10m,z,z_0);
```

```
    wind_speed_relativ=wind_speed_z+Towing_speed_in_ms;
    if i ==1
        Force_D_0(i)=(Steppsize-datapoints_0deg(1,i+1).*(10^2))...
            *datapoints_0deg(3,i+1)*wind_speed_relativ^2;
        Force_L_0(i)=(Steppsize-datapoints_0deg(1,i+1).*(10^2))...
            *datapoints_0deg(2,i+1)*wind_speed_relativ^2;


        Force_D_90(i)=(Steppsize-datapoints_90deg(1,i+1).*(10^2))...
            *datapoints_90deg(3,i+1)*wind_speed_relativ^2;
        Force_L_90(i)=(Steppsize-datapoints_90deg(1,i+1).*(10^2))...
            *datapoints_90deg(2,i+1)*wind_speed_relativ^2;


    else
        Force_D_0(i)=Steppsize...
            *datapoints_0deg(3,i+1)*wind_speed_relativ^2;
        Force_L_0(i)=Steppsize*2 ...
            *datapoints_0deg(2,i+1)*wind_speed_relativ^2;


        Force_D_90(i)=Steppsize...
            *datapoints_90deg(3,i+1)*wind_speed_relativ^2;
        Force_L_90(i)=Steppsize*2 ...
            *datapoints_90deg(2,i+1)*wind_speed_relativ^2;

    end

end

Force_D_90_sum(j)=sum(Force_D_90);
Force_L_90sum(j)=sum(Force_L_90);

Force_L_sum(j)=sum(Force_D_0);
Force_D_sum(j)=sum(Force_D_0);


end
Force_D_90_tot=sum(Force_D_90_sum);
Force_L_90_tot=sum(Force_L_90sum);

Force_L_0_tot=sum(Force_L_sum);
Force_D_0_tot=sum(Force_D_sum);
end
```

B.6 Drift on the turbine

```
function [Fd] = Drift_on_the_turbine(Towing_speed_in_knots,...
    T_0_turbine,H_S,rho_water)
%UNTITLED5 Summary of this function goes here
%   Detailed explanation goes here
g=9.81;
depth=18.3;
D=18.3;
R=D/2;

zeta_a=1;  % enhets bølge (Kjell)
```

```
Towing_speed_in_ms=Towing_speed_in_knots*0.514444;%the towing speed in m/s
omega_0=2*pi/T_0_turbine;
omega_e=omega_0+(omega_0^2)*Towing_speed_in_ms/g;
T_1=2*pi/omega_e;
T_1=0.834*T_0_turbine;

F1_del=[0 0 0.014 0.0285 0.043 0.07     0.129 0.18 0.243 0.3 0.357...
    0.414 0.471];
F1=F1_del.*(0.5*rho_water*g*(zeta_a^2)*D);%
omega_graf=[0.001 0.1 0.2 0.3 0.4 0.5 0.6 0.7 0.8 0.9 1 1.1     1.2];
delta_omega=sqrt(0.1*g/R);

omega_graf.*g./R;

    tel=1;
    for i=omega_graf
        omega=sqrt(omega_graf(tel)*g/R);







    if omega <= 5.24/T_1
        sigma=0.07;
    else
        sigma=0.09;
    end
    Y=exp(-(((0.191*omega*T_1)-1)/(sqrt(2)*sigma))^2);

    S(tel)=155*((H_S^2)/((T_1^4)*(omega^5)))*exp(-944/((T_1^4)*...
        (omega^4)))*((3.3)^(Y));
    tel=tel+1;
    end

    gggg=sum(S);

    Fd=2*sum(delta_omega.*F1.*S);
end
```

B.7 Drag coefficient boat

```
% -------------------------------------------------------------------------
%             MAIN FILE - Calculating the force on the turbine
% -------------------------------------------------------------------------
%
%    Calculate the drag and lift forces acting on the turbine exskluing
%    the blades
%
%
%   Name                Description
% -------------------------------------------------------------------------
%
% -------------------------------------------------------------------------
%
% Programmed:           Martin Mongstad Hope  (November 2020)
% -------------------------------------------------------------------------
function [Fd_boat] = Dragcoeficient_boat(Towing_speed_in_knots,...
```

```
    current_speed)
%UNTITLED5 Summary of this function goes here
%   Detailed explanation goes here

C_d=-27.823155970000000;


Towing_speed_in_ms=Towing_speed_in_knots*0.514444;%the towing speed in m/s
Current_speed_in_ms=current_speed*0.514444;
Current_speed_tot=Towing_speed_in_ms+Current_speed_in_ms;

    Fd_boat=C_d*Current_speed_tot^2;
end
```

B.8 Force on the boat

```
% -------------------------------------------------------------------------
%             MAIN FILE - Calculating the force on the turbine
% -------------------------------------------------------------------------
%
%    Calculate the drag and lift forces acting on the turbine exskluing
%    the blades
%
%
%   Name                Description
% -------------------------------------------------------------------------
%   % z_0=0.01;      %DNV-RP-C205 Terrain roughness parameter table 2-1...
%  worst case open sea with waves

% Wind_speed_at_10m=10; %Avrage wind speed at 10m in m/s
% -------------------------------------------------------------------------
%
% Programmed:           Martin Mongstad Hope  (November 2020)
% -------------------------------------------------------------------------
function [Fd] = Force_on_the_boat(Towing_speed_in_knots,Wind_speed_at_10m)
%UNTITLED5 Summary of this function goes here
%   Detailed explanation goes here

% Towing_speed_in_knots=5; % the towing speed in knots
 Towing_speed_in_ms=Towing_speed_in_knots*0.514444;%the towing speed in m/s
 C_d_wind_boat=-1.757346190e-01;

Wind_speed_avrage_tot=Towing_speed_in_ms+Wind_speed_at_10m;




    Fd=C_d_wind_boat*Wind_speed_avrage_tot^2;
end
```

B.9 Drift on the boat

```
function [Fd] = Drift_on_the_boat(T_0,H_S)
%function [Fd] = Drift_on_the_boat(Towing_speed_in_knots,T_0,H_S)
%UNTITLED5 Summary of this function goes here
%   Detailed explanation goes here

T_1=0.834*T_0;
% delta_omega=0.0276;
load('wave_drift')



    tel=1;
    for i=18:90
        omega=wave_drift(i,2);%.*0.1592;
        if i==18
            delta_omega(tel)=wave_drift(i,2)+((wave_drift(i+1,2)...
                -wave_drift(i,2))/2);
        elseif i==90
            delta_omega(tel)=wave_drift(i,2)-wave_drift(i-1,2);
        else
            delta_omega(tel)=((wave_drift(i+1,2)-wave_drift(i,2))/2)+...
                ((wave_drift(i,2)-wave_drift(i-1,2))/2);
        end




    if omega <= 5.24/T_1
        sigma=0.07;
    else
        sigma=0.09;
    end
    Y=exp(-(((0.191*omega*T_1)-1)/(sqrt(2)*sigma))^2);
    S(tel)=155*((H_S^2)/((T_1^4)*(omega^5)))*exp(-944/((T_1^4)*...
        (omega^4)))*(3.3)^(Y);
    tel=tel+1;
    end

    teller=1;
    for j=970:1042
        Cd_drift_tug(teller)=wave_drift(j,3);
        teller=teller+1;
    end
    period_test=1./(wave_drift(18:90,2).*(1/(2*pi)));
%     figure
%     plot(period_test,S)



    Fd=2*sum(delta_omega.*Cd_drift_tug.*S);
end
```

B.10 Frequncy domain model

```
close all
clear all

DataLoading %loads vessel and weather data



Steelcable4_MBL %loads towing line data
% Steelcable3_MBL_no_curent
% chain1
% chain1_no_curent
% Polyester1
% Polyester1_no_curent



L_line=1800;

Towspeed=2;%knots
opdist=90; %operation distance in Nm
Op_length=(90/Towspeed)*60*60;%Operational time in sec for ...
%2 knots tow speed




x=-0.5*LOA;
%vector calcultions inorder to take into acount phase
Heave_aft_x=RAO_Heave_COG_0deg-((x*RAO_Pitch_COG_0deg).*cosd(PhaseDif));
Heave_aft_y=-(x*RAO_Pitch_COG_0deg).*sind(PhaseDif);
RAO_Heave_aft=sqrt(Heave_aft_x.^2 +Heave_aft_y.^2);%resulting heave...
motion aft



K_E=EA/L_line;
K_G=(12*H^3)/(((W_0*L_line)^2) *L_line);
K_tot=((1/K_E)+(1/K_G))^(-1);







PhaseResult=atand(Heave_aft_x./Heave_aft_y);
T_resonans=2*pi*sqrt((Mass+Added_Mass)/(K_tot));
PhaseDifSurge=Phase_Surge-PhaseResult;
 phi=atan(W_0*(abs(x)/H));
% phi=0.015;
HeaveRelative=(pi/2)-phi;
% SurgeRelative=180-phi;

Surge_along_line=RAO_Surge_COG_0deg*cos(phi);
Heave_along_line=RAO_Heave_aft*cos(HeaveRelative);
motion_line_rel=Surge_along_line-((Heave_along_line).*cosd(PhaseDifSurge));
motion_line_im=-(Heave_along_line).*sind(PhaseDifSurge);
RAO_motion_along_line=sqrt(motion_line_rel.^2 +motion_line_im.^2);
```

```
%resulting heave motion aft

% figure
% plot(freq,RAO_motion_along_line)
% title('Motion along line RAO ')
%  xlabel('\omega [rad/s]')
%  ylabel('$\frac{\eta_{\phi}}{\zeta} \quad$','interpreter','latex','Rotation',0)


RAO_Tension_no_drag_only_Ke=RAO_motion_along_line*K_E;

RAO_Tension_no_drag=RAO_motion_along_line.*K_tot;
%
figure
plot(freq,RAO_Tension_no_drag)
title('Tension in line RAO excluding damping for mild weather')
 xlabel('\omega [rad/s]')
 ylabel('$kN/m$','interpreter','latex','Rotation',0)




T_1=T_0*0.834;%*0.834;%12.2
T_2=T_0*0.834/1.073;
% H_S=6.1;
Towing_speed_in_knots=2;
Towing_speed_in_ms=Towing_speed_in_knots*0.514444;% the towing speed in m/s


    tel=1;
    for i=1:73
        omega=freq(i);%.*0.834;







    if omega <= 5.24/T_1
        sigma=0.07;
    else
        sigma=0.09;
    end
    Y=exp(-((0.191*omega*T_1-1)/(sqrt(2)*sigma))^2);
    S(tel)=155*((H_S^2)/((T_1^4)*(omega^5)))*exp(-944/((T_1^4)*...
        (omega^4)))*(3.3)^(Y);
    tel=tel+1;
    end
  %N=Op_length/T_2;
  N=3*60*60/T_2;
%          figure
%     plot(1./(freq.*(1/(2*pi))),S)
%     title('wave spectrum')

%      figure
%     plot(freq,S)
%     title('wave spectrum')

   S_wave_velocity=abs(transpose(freq)).^2 .*S;
```

```
    m_0_wave=sum(S.*freq_d);
    sigma_wave=sqrt(m_0_wave);
    wave_max=sigma_wave*sqrt(2*log(N));


    m_0_wave_velocity=sum(S_wave_velocity.*freq_d);
    sigma_wave_velocity=sqrt(m_0_wave_velocity);


     Heave_S_towline_motion=abs(transpose(RAO_Heave_COG_0deg)).^2.*S;
    Heave_m_0_towline=sum(Heave_S_towline_motion.*freq_d);
    Heave_sigma_towline=sqrt(Heave_m_0_towline);
     Heave_towline_motion_max=Heave_sigma_towline*sqrt(2*log(N));

     Heaveaft_S_towline_motion=abs(transpose(RAO_Heave_aft)).^2.*S;
    Heaveaft_m_0_towline=sum(Heaveaft_S_towline_motion.*freq_d);
    Heaveaft_sigma_towline=sqrt(Heaveaft_m_0_towline);
     Heaveaft_towline_motion_max=Heaveaft_sigma_towline*sqrt(2*log(N));

    Surge_S_towline_motion=abs(transpose(RAO_Surge_COG_0deg)).^2.*S;
    Surge_m_0_towline=sum(Surge_S_towline_motion.*freq_d);
    Surge_sigma_towline=sqrt(Surge_m_0_towline);
     Surge_towline_motion_max=Surge_sigma_towline*sqrt(2*log(N));









     Pitch_S_towline_motion=abs(transpose(RAO_Pitch_COG_0deg)).^2.*S;
    Pitch_m_0_towline=sum(Pitch_S_towline_motion.*freq_d);
    Pitch_sigma_towline=sqrt(Pitch_m_0_towline);
     Pitch_towline_motion_max=Pitch_sigma_towline*sqrt(2*log(N));


    S_towline_motion=abs(transpose(RAO_motion_along_line)).^2.*S;
    m_0_towline=sum(S_towline_motion.*freq_d);
    sigma_towline=sqrt(m_0_towline);
     S_towline_motion_max=sigma_towline*sqrt(2*log(N));

       figure
    plot(freq,S_towline_motion)
    title('Towline motion sepectrum for mild weather')
        xlabel('\omega [rad/s]')
    ylabel('$m^2s$','interpreter','latex','Rotation',0)



%      figure
%     plot(freq,S_towline_motion)
%     title('Towline spectrum')

    S_towline_velocity=abs(transpose(freq)).^2 .*S_towline_motion;
    m_0_towline_velocity=sum(S_towline_velocity.*freq_d);
    sigma_towline_velocity=sqrt(m_0_towline_velocity);


%
```

```
%     figure
%     plot(freq,S_towline_velocity)
%     title('Towline velocity spectrum')
%
%     figure
%     plot(freq,S)
%     title('Wave spectrum')

    %%%%%%%%%%%%%%%%%%%%%%%%%%%%%%%%%%%%

    S_tension_no_drag=abs(transpose(RAO_Tension_no_drag)).^(2) .*S;

%     figure
%     plot(freq,S_tension_no_drag)
%     title(' spectrum no drag ')

    m_0_tension_no_drag=sum(S_tension_no_drag.*freq_d);
    sigma_tension_no_drag=sqrt(m_0_tension_no_drag);
    significatn_value_responce_tension_no_drag=4*sqrt(m_0_tension_no_drag);


   T_dyn_max_no_drag=sigma_tension_no_drag*sqrt(2*log(N));

    %%%%%%%%%%%%%%%%%%%%%%%%%%%%%%%%%%%%
    S_tension_no_drag_only_Ke=abs(transpose...
        (RAO_Tension_no_drag_only_Ke)).^(2) .*S;
%
%     figure
%     plot(freq,S_tension_no_drag_only_Ke)
%     title(' spectrum no drag only Ke ')

    m_0_tension_no_drag_only_Ke=sum(S_tension_no_drag_only_Ke.*freq_d);
    sigma_tension_no_drag_only_Ke=sqrt(m_0_tension_no_drag_only_Ke);
    significatn_value_responce_tension_no_drag_only_Ke=4*sqrt...
        (m_0_tension_no_drag_only_Ke);

    %N=Op_length/T_1;
    T_dyn_max_no_drag_only_Ke=sigma_tension_no_drag_only_Ke*sqrt(2*log(N));









T_onlyE_NoD=[T_dyn_max_no_drag_only_Ke T_dyn_max_no_drag H];
```

```
%Drag calculations



Z_m=(W_0*L_line^2)/(8*H);
K_D=0.5*rho_w*10^3*C_d_towline*d_towline;

K_G_old=K_G;


sigma_u_velocity=0;
sigma_u_velocity_new=1;

C_e=0;
C_e_new=1;
sigma_u_i=sigma_towline*(K_E/(K_E*K_G_old));
% i=1;
while (abs(sigma_u_velocity-sigma_u_velocity_new)>0.00001)...
        &&(abs(C_e-C_e_new) >0.00001 )


sigma_u=sigma_towline*(K_E/(K_E+K_G_old));
sigma_u_velocity=sigma_towline_velocity*(K_E/(K_E+K_G_old));

C_e=(1/16)*K_D*K_G_old*(L_line/W_0)*(sqrt(8/pi))*sigma_u_velocity;
C_e_test=0.1*K_D*K_G_old*(L_line/W_0)*sigma_u_velocity;
% C_e-C_e_test;
% U_a=K_E/(K_E+((C_e*)^(2)+()^(2))^(0.5))


f_cor=(sqrt(((C_e*sigma_u_velocity)^(2)+(K_G_old*sigma_u)^(2))))/...
    (K_G_old*sigma_u_i);




% T(i)=f_cor;
% i=i+1;

K_G_new=K_G_old*f_cor;
sigma_u_new=sigma_towline*(K_E/(K_E+K_G_new));
sigma_u_velocity_new=sigma_towline_velocity*(K_E/(K_E+K_G_new));
C_e_new=(1/16)*K_D*K_G_new*(L_line/W_0)*(sqrt(8/pi))*sigma_u_velocity_new;



K_G_old=K_G_new;
end

% figure
% plot(T(2:end))

RAO_tension_cable_motion_drag=K_E.*(1.-(K_E./(K_E+...
    (((C_e_new.*freq_t).^(2)+(K_G).^(2)).^(0.5)))));

K_tot_plot=ones(1,length(freq))*K_tot;
K_E_plot=ones(1,length(freq))*K_E;
```

```
RAO_Tension_wave_drag=RAO_tension_cable_motion_drag.*transpose...
    (RAO_motion_along_line);

  S_tension_drag=abs((RAO_tension_cable_motion_drag.*transpose...
      (RAO_motion_along_line))).^(2) .*S;

    m_0_tension_drag=sum(S_tension_drag.*freq_d);
    sigma_tension_drag=sqrt(m_0_tension_drag);
    significatn_value_responce_tension_drag=4*sqrt(m_0_tension_drag);
    T_dyn_max_drag=sigma_tension_drag*sqrt(2*log(N));




%
sigma_list=[sigma_tension_no_drag_only_Ke,sigma_tension_no_drag,...
    sigma_tension_drag];
T_onlyE_NoD_drag_H=[T_dyn_max_no_drag_only_Ke T_dyn_max_no_drag...
    T_dyn_max_drag H];
```

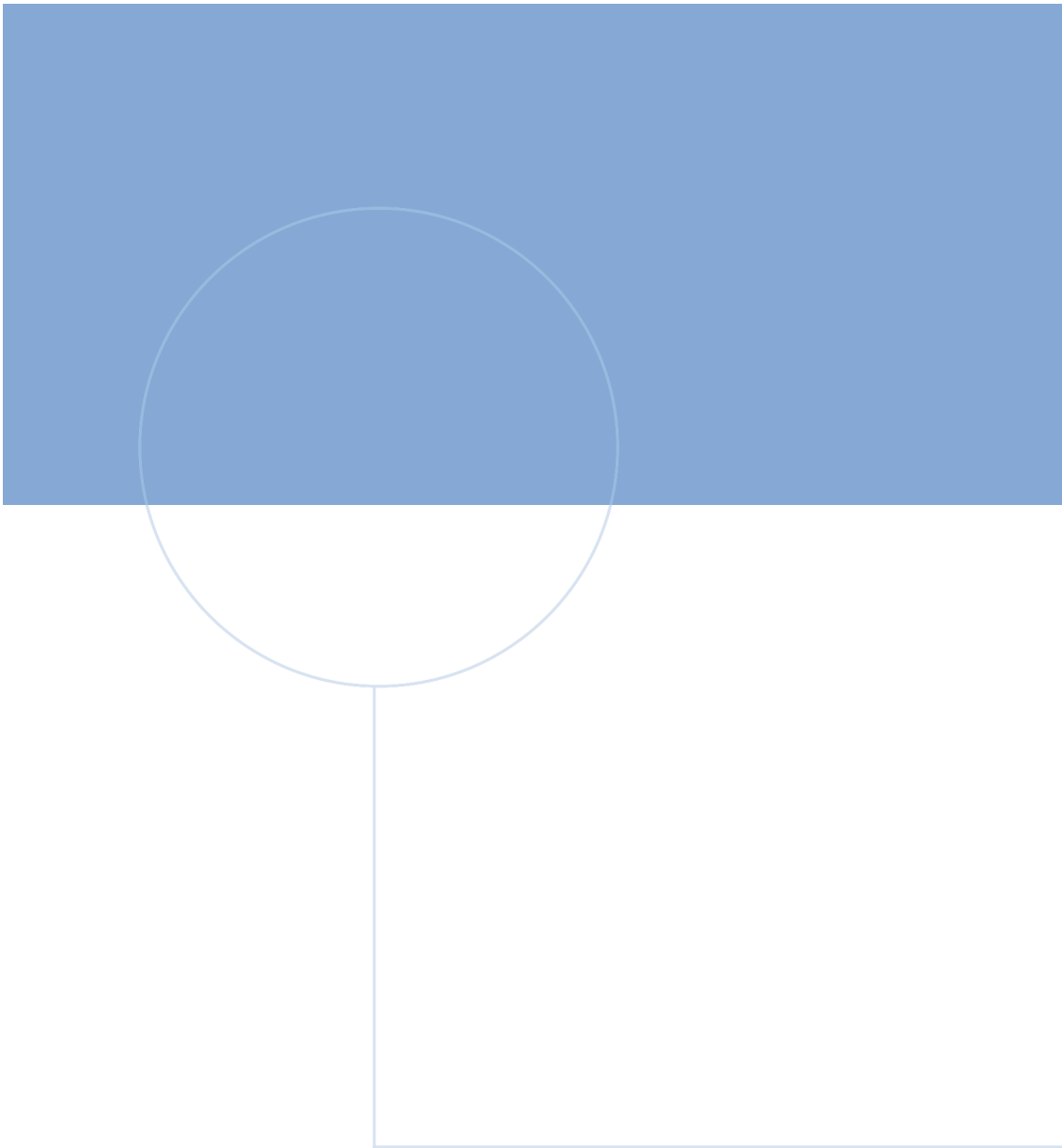

NTNU

Norwegian University of
Science and Technology